blasts, and fibrocytes and may participate in the progression of liver fibrosis.

The present study was designed to reexamine the possible contribution of BM-derived cells to type I collagen production during the progression of liver fibrosis. For this purpose, we utilized 2 mechanistically distinct liver fibrosis models, which were introduced into transgenic collagen reporter mice and their BM recipients. With careful consideration for the experimental design and the qualified methods with high specificity and sensitivity, we conclude that BM-derived cells play an unexpectedly limited role in collagen production during hepatic fibrogenesis. The present study gives a caution to the current growing feeling that overestimates the participation of BM-derived cells in the progression of liver fibrosis.

Materials and Methods

Mice

All animals used in the present study received humane care, and the experiments were approved by the Animal Experiment Committee of Tokai University. C57BL/6 mice were purchased from CLEA Japan Inc. (Tokyo, Japan). A transgenic mouse strain (COL/LUC) that contains the −17,000 to +54 region of the mouse upstream sequence of α2(I) collagen gene (*COL1A2*) linked to a firefly *luciferase* gene was previously described.[14] The −17,000 to −15,450 *COL1A2* sequence exhibits a strong enhancer activity that directs tissue-specific gene expression during embryonic development as well as in adult mouse organs.[14,15] This tissue-specific enhancer and the −350 to +54 minimal *COL1A2* promoter sequences with appropriate linker fragments were cloned into a *Bam*HI site of an EGFP expression plasmid: pEGFP-1 (Clontech Laboratories, Palo Alto, CA). The chimeric DNA fragment was excised from the plasmid to generate transgenic mice (COL/EGFP) that express EGFP exclusively in type I collagen-producing cells. Injection of the purified DNA fragment into fertilized eggs and screening of mice for the presence of transgene were performed as previously described.[14] We established 2 strains of transgenic COL/EGFP mice, which contained approximately 10 and 5 copies of transgene, respectively. Both strains of mice exhibited essentially the same results in the experiments shown in the present study except for the difference in the intensities of EGFP signals. Mice of F3 to F5 generation were used in all of the experiments. Transgenic mice that ubiquitously express EGFP by the cytomegalovirus enhancer and the chicken β-actin promoter (CAG/EGFP) were reported previously.[16]

BM Transplantation

A combination of donor and recipient mice in BM transplantation experiments is illustrated in Figure 1. Transgenic CAG/EGFP, COL/EGFP, and COL//LUC mice were used as BM donors, whereas C57BL/6 wild-type animals were used as recipients. Transplantation of unfractionated whole BM cells including hematopoietic

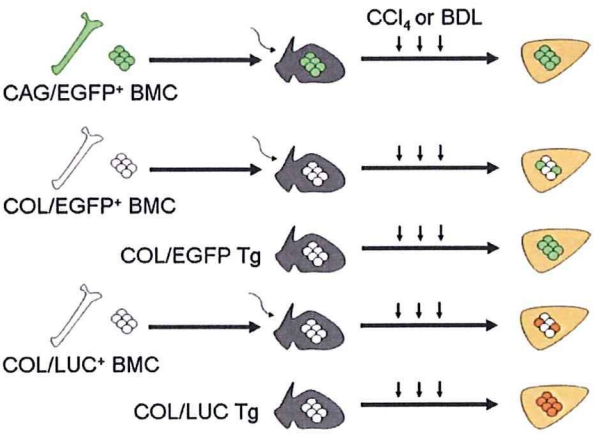

Figure 1. Schematic representation of a combination of donor and recipient mice used in bone marrow transplantation experiments. Whole bone marrow cells (*BMC*) obtained from transgenic CAG/EGFP, COL/EGFP, or COL/LUC mice were injected into the irradiated C57BL/6 wild-type animals. Those recipient mice received subcutaneous injections of 1 mL/kg body weight of carbon tetrachloride (CCl_4) every 3 days for a total of 30 times or underwent ligation of the common bile duct (CBD). Transgenic COL/EGFP and COL/LUC mice (*Tg*) were also included as controls.

stem cells to the irradiated recipient mice was performed as previously described.[3] Engraftment of donor cells was confirmed 6 weeks after BM transplantation by fluorescence-activated cell-sorter scanner (FACS) analyses of EGFP-expressing cells in the peripheral blood of CAG/EGFP recipient mouse or by polymerase chain reaction (PCR) detection of *EGFP* and *luciferase* transgenes in the spleen tissue of COL/EGFP and COL/LUC recipients (Supplementary Figure 1), respectively.

Induction of Liver Fibrosis

Eight weeks after transplantation, BM-recipient mice, as well as transgenic CAG/EGFP, COL/EGFP, and COL/LUC animals, started to be injected subcutaneously with 1 mL/kg body weight of CCl_4 mixed with olive oil every 3 days for a total of 30 times[17] or underwent ligation of the common bile duct (CBD).[18] Three to 4 mice in each group of transgenic mice and their BM recipients were killed 48 hours after the last CCl_4 injection or 14 days after CBD ligation.

Isolation of HSC and FACS Analysis

Murine HSC were isolated by using the collagenase-pronase perfusion method as previously described[19] and subjected to FACS analyses. Presence of EGFP-positive cells in the freshly isolated HSC fraction, peripheral blood, and BM was analyzed by using FACS Calibur flow cytometer (Becton Dickinson, San Jose, CA).

Confocal Microscopic Examination

Migration of EGFP-expressing cells into fibrotic liver was viewed and analyzed by a confocal laser-scanning microscope: LSM 510 META (Carl Zeiss, Jena, Ger-

many). The emission fingerprinting method[20] was utilized, which distinguished specific fluorescent signals from the background autofluorescence as previously described.[3] EGFP-expressing cells observed in the liver of CAG/EGFP-recipient mice indicate the BM origin irrespective of their phenotypes, whereas those detected in COL/EGFP recipients represent exclusively BM-derived collagen-producing cells migrating into fibrotic liver. Transgenic COL/EGFP mice were also used as a control, showing collagen-expressing cells in the liver irrespective of their origins. Immunohistochemical or immunofluorescence staining was performed as previously described[3] with antibodies against type I collagen (Calbiochem, San Diego, CA), α-smooth muscle actin (α-SMA) (Sigma Chemical Co, St. Louis, MO), and F4/80 (Serotec, Raleigh, NC).

Luciferase Assay

Liver samples obtained from COL/LUC-recipient mice were subjected to luciferase assays to evaluate activation of *COL1A2* promoter in BM-derived cells migrating into fibrotic liver. Transgenic COL/LUC mice were also used as a control to quantify *COL1A2* promoter activity in the liver before and after fibrogenic stimuli. Luciferase assays of liver tissue were performed as previously described,[17,21] and the enzyme activity was normalized against the protein concentration of tissue homogenates.

Statistical Analysis

Values were expressed as mean ± SD. The Mann–Whitney *U* test was used to evaluate the statistical differences between groups: a *P* value of less than .05 was considered statistically significant.

Results

BM-Derived Cells Migrating Into Fibrotic Liver Seldom Differentiate Into α-SMA-Positive Cells in Both Experimental Fibrosis Models

We first examined migration of BM cells into liver tissue in 2 mechanistically distinct fibrosis models introduced into CAG/EGFP-recipient mice. As previously reported,[3] bridging fibrosis connecting the neighboring portal areas and central veins was formed, but complete cirrhosis was not established after 30 times of repeated CCl_4 injections (Figure 2*A*). A large number of EGFP-expressing BM-derived cells migrated into the fibrotic liver 2 days after the last CCl_4 injection, at peak fibrosis (Figure 2*B*). On the other hand, CBD ligation resulted in the accumulation of collagen fibers underneath the dilated and proliferating bile duct epithelium 14 days after the operation (Figure 2*C*). EGFP-expressing BM-derived cells were observed mainly in those fibrotic areas around the dilated bile ducts as well as within the liver parenchyma (Figure 2*D*). However, immunostaining of type I collagen failed to determine precisely whether the EGFP-positive cells present in the fibrous tissue certainly produce collagen or whether they were merely surrounded by collagen fibers (Figure 3*A*). In addition, although EGFP-expressing BM-derived cells and α-SMA-positive cells exhibited the similar distribution following repeated CCl_4 injections (Figure 3*B*) and CBD ligation (Figure 3*C*), they seldom overlapped each other (Figure 3*D*). Three-dimensional confocal microscopic analyses estimated that the mean number of BM-derived α-SMA-positive cells was less than a single cell per each portal area (Figure 3*E*).

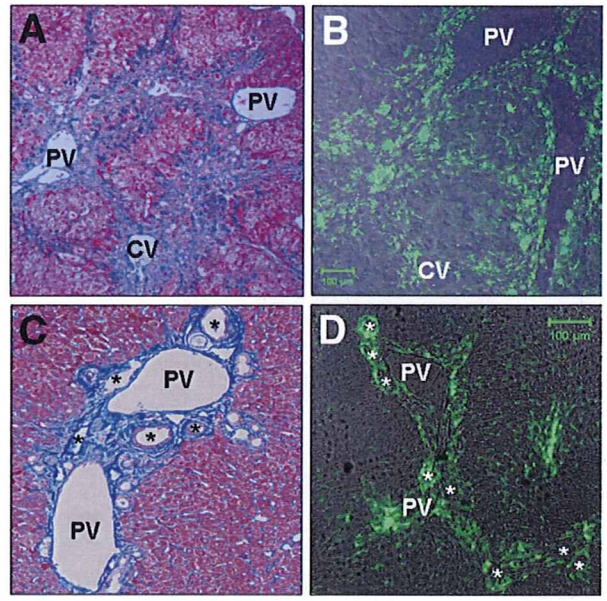

Figure 2. Migration of BM-derived cells into fibrotic liver. Liver specimens were obtained from CAG/EGFP recipient mice following 30 times of repeated CCl_4 injections (*A* and *B*) or 14 days after common bile duct (CBD) ligation (*C* and *D*). The sections were subjected to Azan-Mallory staining (*A* and *C*) or confocal laser-scanning microscopic examination detecting EGFP-positive cells (*green* in *B* and *D*). Representative pictures are shown from 3 to 4 mice in each group. Note that the bile duct epithelial cells do not express EGFP. *Asterisks* indicate dilated bile ducts around the portal vein. *PV*, portal vein; *CV*, central vein. Original magnification, 40× in *A* or 100× in *C*. *Scale bars*, 100 μm in *B* and *D*.

EGFP Expression Driven by the Tissue-Specific COL1A2 *Enhancer Is Stimulated Following Fibrogenic Stimuli in Vivo and During Primary Culture in Vitro*

Next, we examined cell type-specific expression of EGFP driven by the *COL1A2* enhancer. For this purpose, transgenic COL/EGFP mice were first treated with a single dose of CCl_4. Our previous study using transgenic mice that harbor the same tissue-specific *COL1A2* enhancer/promoter sequence linked to a firefly *luciferase* gene (COL/LUC) indicated that *COL1A2* promoter was activated more than 10-fold 72 hours after a single CCl_4 injection.[21] Confocal microscopic examination of excised liver tissue showed a significant number of EGFP-expressing cells present in the centrilobular necrotic areas 48 hours after CCl_4 administration (compare Figure 4*A*

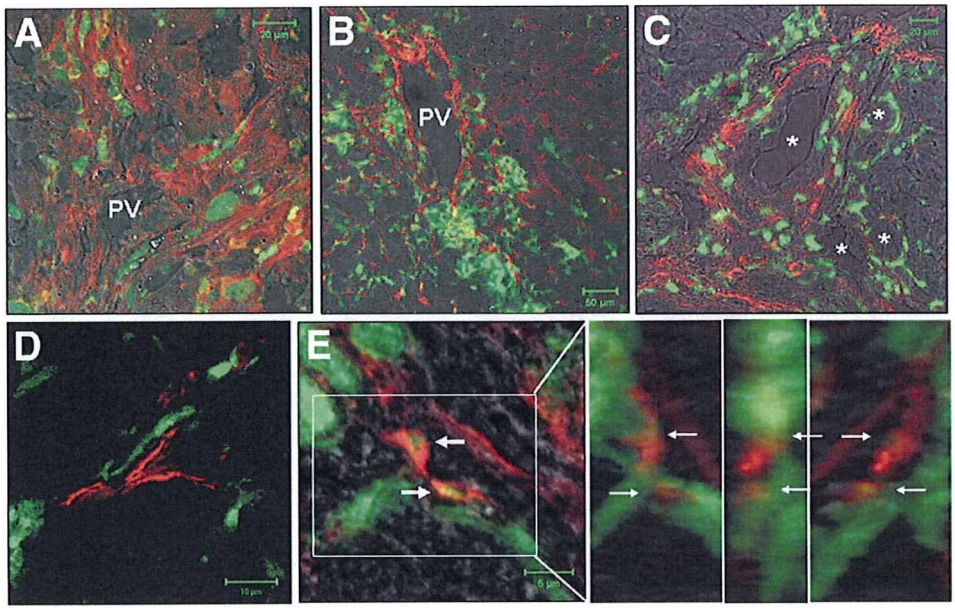

Figure 3. Expression of type I collagen and α-SMA in BM-derived *cells* migrating into fibrotic liver. Liver specimens were obtained from CAG/EGFP-recipient mice following 30 times of repeated CCl_4 injections (*A*, *B*, *D*, and *E*) or 14 days after CBD ligation (*C*). The sections were stained with specific antibodies recognizing type I collagen (*red* in *A*) or α-SMA (*red* in *B–E*). In *panel E* is shown a 3-dimensional rotation analysis of 2 EGFP-positive cells (*arrows*) that coexpress α-SMA. Representative pictures are shown from 3 to 4 mice in each group. *Asterisks* indicate dilated bile ducts. *PV*, portal vein. *Scale bars* are shown in each *panel*.

and *B*). They exhibited a mesenchymal morphology, and none of the parenchymal hepatocytes expressed EGFP. Immunofluorescence studies indicated that approximately half of EGFP-expressing cells were positive for α-SMA, a marker of activated HSC (Figures 4*C* and *D*). In contrast, none of the EGFP-expressing cells were positive for F4/80, a marker of macrophage/Kupffer cells (Figures 4*E* and *F*). FACS analyses indicated that 28.7% ± 1.8% of HSC isolated from CCl_4-treated transgenic COL/EGFP mice were positive for EGFP. Activation of *COL1A2* promoter was also examined in primary culture of HSC obtained from untreated transgenic COL/EGFP mice. Whereas quiescent HSC at day 2 after plating on plastic showed no EGFP fluorescence (data not shown), strong EGFP fluorescence was observed in activated cells at day 7, which was coexpressed with endogenous type I collagen (Figure 5*A*) and α-SMA (Figure 5*B*).

COL1A2 *Promoter Activation Attributes to Liver Resident Cells but not BM-Derived Cells*

After confirming the cell type-specific activation of *COL1A2* promoter, we next examined whether the

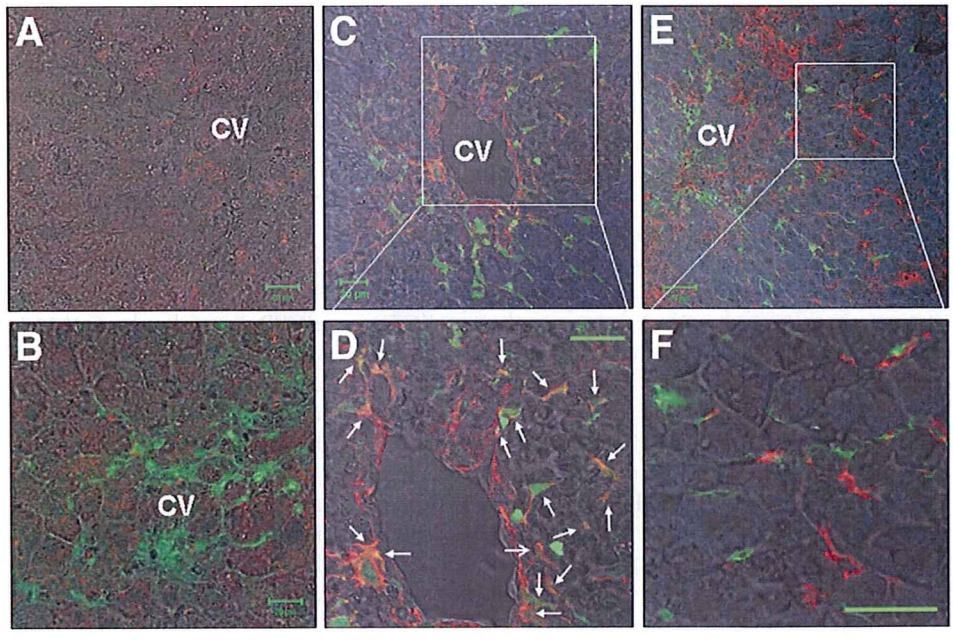

Figure 4. Activation of *COL1A2* promoter following CCl_4 administration. Expression of EGFP (*green*) was examined in liver specimens obtained from wild-type (*A*) or transgenic COL/EGFP mice (*B–F*) 72 hours after a single CCl_4 injection. The sections were stained with specific antibodies recognizing α-SMA (*red* in *C* and *D*) or F4/80 (*red* in *E* and *F*). Representative pictures are shown from 4 mice in each group. *Arrows* indicate EGFP-positive cells that coexpress α-SMA. *CV*, central vein. *Scale bars*, 20 μm in *A–D* or 50 μm in *E* and *F*.

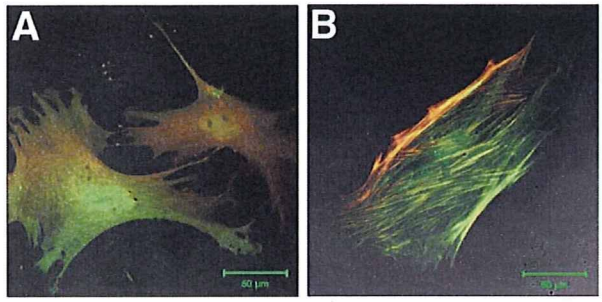

Figure 5. Expression of type I collagen and α-SMA in culture-activated stellate cells. Hepatic stellate cells were obtained from untreated transgenic COL/EGFP mice and subjected to primary culture on plastic for 7 days. Coexpression of EGFP (*green*) and type I collagen (*red* in *A*) or α-SMA (*red* in *B*) was examined by immunofluorescence studies using specific antibodies. Representative pictures are shown from 3 mice. *Scale bars*, 50 μm.

promoter was activated in BM-derived cells or in liver resident cells following fibrogenic stimuli. For this purpose, 2 mechanistically distinct models of liver fibrosis were introduced into transgenic COL/EGFP and COL/LUC mice or their BM-recipient mice. By comparing EGFP expression and luciferase activities between transgenic mice and their BM recipients, we can estimate how each population of BM-derived cells and liver resident cells contributes to collagen production and thus participates in the progression of liver fibrosis. There was no difference between transgenic mice and their BM recipients in the degree of liver fibrosis introduced by repeated CCl_4 injections or CBD ligation (data not shown). A large number of EGFP-positive cells were observed in the portal areas and along the fibrous septa after repeated CCl_4 injections into transgenic COL/EGFP mice, and most of the EGFP-expressing cells were positive for α-SMA staining (Figure 6*A*). On the other hand, coexpression of EGFP and α-SMA was detected in mesenchymal cells present underneath the dilated and proliferating bile duct epithelium after CBD ligation (Figure 6*C*). In contrast, there were few, if any, EGFP-positive BM-derived collagen-expressing cells detected in fibrotic liver tissue of COL/EGFP-recipient mice following either CCl_4 injections (Figure 6*B*) or CBD ligation (Figure 6*D*). Furthermore, as shown in the previous studies,[17,21] luciferase assays of liver tissue revealed that *COL1A2* promoter was activated more than 5-fold following repeated CCl_4 injections into transgenic COL/LUC mice (Figure 7). Similar extent of promoter activation was observed in liver tissue 14 days after CBD ligation (Figure 7). In contrast, *COL1A2* promoter was not activated in liver tissue of COL/LUC-recipient mice. The luciferase enzyme activities in liver tissue of COL/LUC-recipient mice were as low as those in wild-type animals following either CCl_4 injections or CBD ligation (Figure 7). These results clearly indicate that activation of *COL1A2* promoter attributes to liver resident cells, but not BM-derived cells, in both of the 2 mechanistically distinct models of liver fibrosis.

COL1A2 *Promoter Is Not Activated in BM Cells Following Fibrogenic Stimuli*

In the last set of experiments, we examined whether fibrogenic stimuli enhanced *COL1A2* promoter activity in BM cells. FACS analyses indicated that a small population (0.23% ± 0.02%) of BM cells isolated from untreated COL/EGFP reporter mice was positive for EGFP. However, there was no increase in the EGFP-positive ratio of BM cells from transgenic COL/EGFP mice following CCl_4 injections (0.19% ± 0.09%) or BDL (0.20% ± 0.04%). Similarly, there was no difference in the luciferase activities in BM cells isolated from transgenic COL/LUC mice before and after fibrogenic stimuli (data not shown).

Discussion

In the present study, we have revealed an unexpectedly limited role of BM-derived cells in collagen production in 2 mechanistically distinct models of liver fibrosis. Although some of the BM-derived cells exhibited a mesenchymal morphology resembling myofibroblasts, the number of BM-derived α-SMA-positive cells was much smaller than previously reported. More importantly, specific and quantitative analyses of *COL1A2* promoter activation by using a combination of *EGFP* and *luciferase* reporter genes have clearly indicated that BM-derived cells produce little, if any, type I collagen during hepatic fibrogenesis.

There have been a large number of studies showing that BM-derived stem/progenitor cells contribute to the repair of severely injured liver either through transdifferentiation into parenchymal hepatocytes or by cell fusion with liver resident cells. However, the frequency of those phenomena is usually very low.[22] Instead, BM-derived cells often differentiate into a mesenchymal lineage. Several recent studies have indicated that BM-derived cells express MMPs and contribute to the regression of experimental liver fibrosis via mobilization from BM[3] or following a therapeutic cell infusion.[23–25] Based on the results of those experimental studies, there have been an increasing number of clinical trials to treat patients with various liver diseases by infusing either whole or fractionated autologous BM cells.[4–8] On the other hand, several experimental and human studies have reported that BM cells differentiate into HSC,[11,13] myofibroblasts,[9,10] and fibrocytes[12] and may participate in liver fibrosis. These findings are in agreement with the results of a number of studies showing functional contribution of blood-borne collagen-producing cells to tissue repair or fibrosis in various other organs.[26–28] They also give a serious caution that BM-derived cells possess both pro- and anti-fibrotic phenotypes.[29]

However, direct contribution of BM-derived cells to collagen production during hepatic fibrogenesis has not been fully verified for the following critical reasons. First, previous studies employed several different methods to identify the BM origin, such as fluorescence in situ hy-

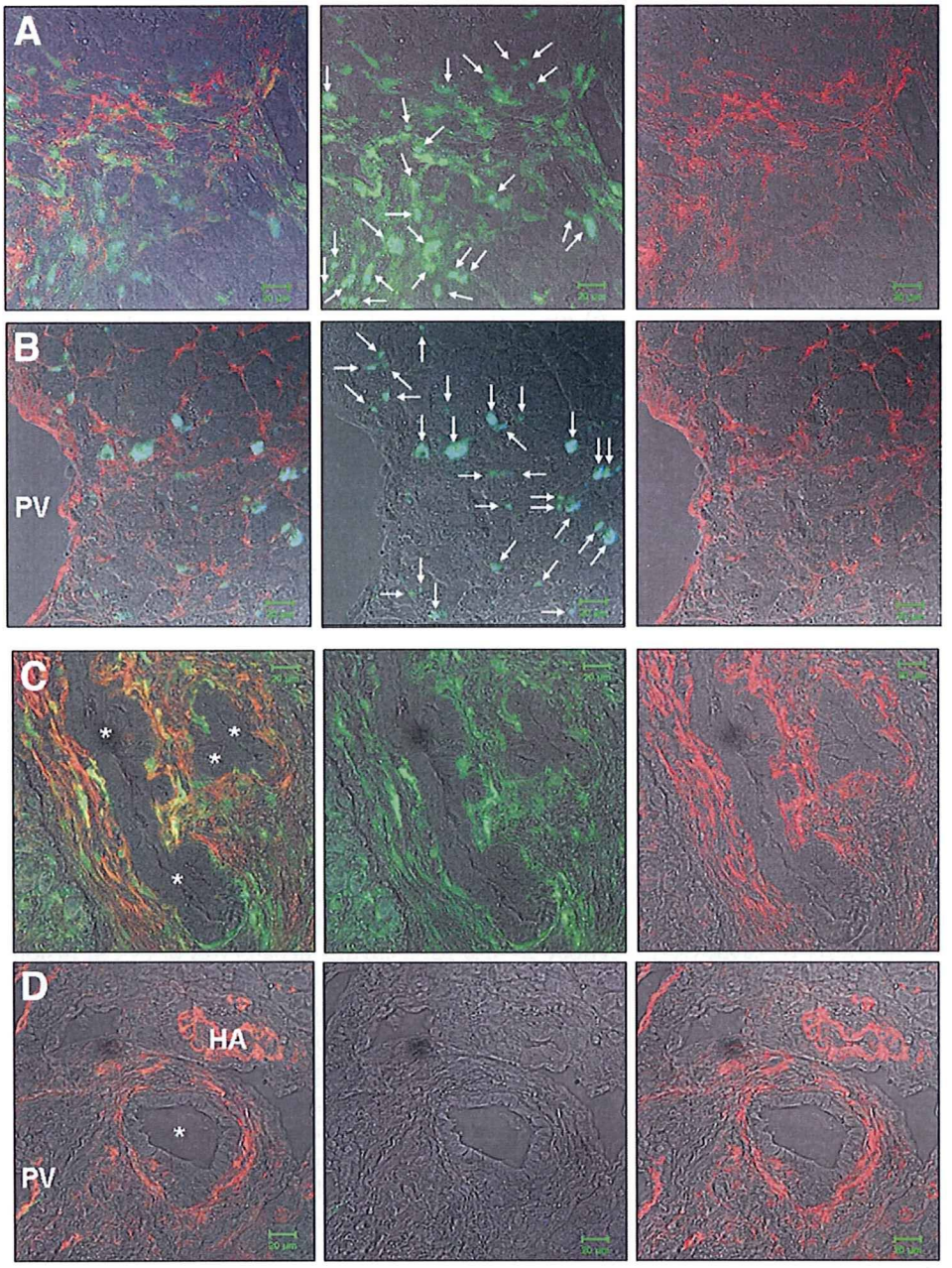

Figure 6. Activation of *COL1A2* promoter in BM-derived cells and liver resident cells. Expression of EGFP (*green*) was examined in liver specimens from transgenic COL/EGFP mice (*A* and *C*) or their BM recipients (*B* and *D*) following 30 times of repeated CCl_4 injections (*A* and *B*) or 14 days after CBD ligation (*C* and *D*). The sections were stained with specific antibodies recognizing α-SMA (*red*). In the *middle* and *right panels* are shown the images of only EGFP and autofluorescence (*middle*) and α-SMA (*right*), respectively. Representative pictures are shown from 3 to 4 mice in each group. Note that the pale signals (*arrows*) observed in *panels A* and *B* represent nonspecific autofluorescence but not the specific EGFP signals. *Asterisks* indicate dilated bile ducts. *PV*, portal vein; *HA*, hepatic artery. *Scale bars*, 20 μm.

bridization technique to detect Y chromosomes[9,10] and immunohistochemical staining of EGFP.[11–13] However, the quality of the employed methods and obtained results was not always enough in terms of both specificity and sensitivity. Second, it is difficult to prove collagen production by BM-derived cells present within the fibrous tissue because of an abundant amount of extracellular collagen accumulated around the cells (Figure 3*A*). Therefore, most of the previous studies failed to demonstrate clearly collagen production by BM-derived cells and relied primarily on the presence of myofibroblast-like cells in the fibrous tissue and their expression of α-SMA.[9–11] Finally, and in relation to the second issue, even if some of the cells exhibit the feature of α-SMA-positive myofibroblasts, it does not necessarily mean that they certainly produce collagen and contribute directly to the progression of liver fibrosis.[30] The cellular entity of BM-derived collagen-producing cells, if present, has not been established yet.

Considering the limitations in the previous studies described above, we tried in the present study to evaluate the direct contribution of BM-derived cells to collagen production by using more specific and quantitative methods. To identify only the specific EGFP fluorescence, we utilized in the previous and present studies the emission fingerprinting method,[3] which successfully elimi-

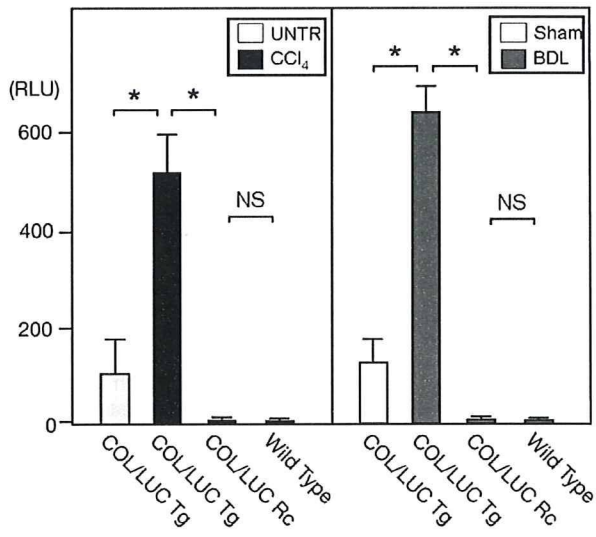

Figure 7. Quantitative analysis of *COL1A2* promoter activation following fibrogenic stimuli. Transgenic COL/LUC mice (*Tg*) and their BM recipients (*Rc*) as well as wild-type animals received repeated CCl_4 injections for a total of 30 times or underwent CBD ligation. They were killed 48 hours after the last CCl_4 injection or 14 days after CBD ligation, and obtained liver tissue was subjected to luciferase assays determining *COL1A2* promoter activity. Liver specimens from untreated (*UNTR*) or sham-operated mice were also analyzed as controls. Luciferase activity was normalized against the protein concentration of tissue homogenates. The values are mean ± SD obtained from 4 mice in each group. The *asterisk* indicates that the difference between the groups is significant. *RLU*, relative luminescence units; *NS*, not significant.

nated the background autofluorescence (Figure 6*A* and *B*). Moreover, we used a firefly *luciferase* gene driven by a tissue-specific *COL1A2* enhancer sequence. Strong tissue specificity of the enhancer that is activated exclusively in collagen-producing cells,[14,15] coupled with the use of sensitive *luciferase* gene as a reporter, engaged a highly specific and quantitative analysis of promoter activation.[21] By using COL/LUC-recipient mice, we demonstrated a complete lack of *COL1A2* promoter activation in BM-derived cells following fibrogenic stimuli.

On the other hand, experiments using transgenic reporter mice also possess several limitations. For example, EGFP is known to be sometimes cytotoxic,[31] and one may argue that BM-derived collagen-producing cells cannot survive for a long time while leaving a large amount of collagen in fibrotic tissue. However, cells with strong EGFP signals were observed in fibrotic liver tissue of CAG/EGFP-recipient mice (Figure 2*B* and *D*) and transgenic COL/EGFP animals (Figure 6*A* and *C*). In addition, the results of parallel experiments using the *luciferase* gene as another reporter (Figure 7) also excluded such a concern. Another limitation of transgenic mouse study is that the expression levels of transgene may vary even by using the same enhancer/promoter sequence. In addition, there is always a chance that the used enhancer/promoter sequence lacks a regulatory element and may not label the entire collagen-expressing populations in the mouse. It should be noted, however, that exactly the same COL/LUC reporter mice and their BM recipients as the present study have been utilized to determine the functional contribution of BM-derived cells to collagen production in various other organs. One of such studies clearly indicated that the luciferase activity in BM-derived cells was dramatically increased in the scar area following experimental myocardial infarction.[28] Our recent study using the same mice also showed a limited but significant amount of collagen produced by BM-derived cells during bleomycin-induced dermal fibrosis (Higashiyama et al, manuscript submitted). On the other hand, an experiment using the same COL/LUC mice failed to demonstrate the contribution of BM-derived cells to collagen production in renal fibrosis induced by a unilateral ureteric obstruction.[32] Collectively, it could be argued that the extent of contribution of BM-derived cells to collagen production may vary depending on the etiologies of tissue injury and/or the sites of affected organs.

The results of the present study do not deny completely the production of type I collagen by BM-derived cells in certain experimental and clinical conditions, depending on the etiologies, severity, and stages of liver fibrosis. However, we excluded their contribution to collagen production in 2 mechanistically distinct models of liver fibrosis. In addition, we also tested at an earlier stage of liver fibrosis induced by 10 times of CCl_4 injections but did not find any evidence for collagen production by BM-derived cells (Supplementary Figure 2).

The localization of BM-derived EGFP-positive cells shown in Figure 2 was almost entirely associated with the fibrotic areas. Although functional properties of the majority of those cells have not been defined yet, our previous study demonstrated that some of them were hematopoietic progenitor cells and inflammatory cells such as neutrophils and macrophages.[3] The present study showed that none of them expressed collagen or α-SMA, but the latter types of cells may participate in the progression of liver fibrosis by secreting several inflammatory cytokines. Further studies are necessary to reveal the functional cross talk between the BM-derived cells and liver resident collagen-producing cells.

In conclusion, this study has clearly revealed a limited role of BM-derived cells in collagen production during hepatic fibrogenesis. The BM origin of cells has to be determined much more carefully, and the results of the present study give a caution to the current growing feeling that overestimates the participation of BM-derived cells to collagen production during the progression of liver fibrosis.

Supplementary Data

Note: To access the supplementary material accompanying this article, visit the online version of *Gastroenterology* at www.gastrojournal.org, and at doi: 10.1053/j.gastro.2009.07.006.

References

1. Friedman SL. Cellular sources of collagen and regulation of collagen production in liver. Semin Liver Dis 1990;10:20–29.
2. Watanabe T, Niioka M, Hozawa S, et al. Gene expression of interstitial collagenase in both progressive and recovery phase of rat liver fibrosis induced by carbon tetrachloride. J Hepatol 2000; 33:224–235.
3. Higashiyama R, Inagaki Y, Hong YY, et al. Bone marrow-derived cells express matrix metalloproteinases and contribute to regression of liver fibrosis in mice. Hepatology 2007;45:213–222.
4. am Esch JS II, Knoefel WT, Klein M, et al. Portal application of autologous $CD133^+$ bone marrow cells to the liver: a novel concept to support hepatic regeneration. Stem Cells 2005;23: 463–470.
5. Gordon MY, Levicar N, Pai M, et al. Characterization and clinical application of human $CD34^+$ stem/progenitor cell populations mobilized into the blood by granulocyte colony-stimulating factor. Stem Cells 2006;24:1822–1830.
6. Terai S, Ishikawa T, Omori K, et al. Improved liver function in patients with liver cirrhosis after autologous bone marrow cell infusion therapy. Stem Cells 2006;24:2292–2298.
7. Gasbarrini A, Rapaccini GL, Rutella S, et al. Rescue therapy by portal infusion of autologous stem cells in a case of drug-induced hepatitis. Dig Liver Dis 2007;39:878–882.
8. Lyra AC, Soares MB, da Silva LF, et al. Feasibility and safety of autologous bone marrow mononuclear cell transplantation in patients with advanced chronic liver diseases. World J Gastroenterol 2007;13:1067–1073.
9. Forbes SJ, Russo FP, Rey V, et al. A significant proportion of myofibroblasts are of bone marrow origin in human liver fibrosis. Gastroenterology 2004;126:955–963.
10. Russo FP, Alison MR, Bigger BW, et al. The bone marrow functionally contributes to liver fibrosis. Gastroenterology 2006;130: 1807–1821.
11. Baba S, Fujii H, Hirose T, et al. Commitment of bone marrow cells to hepatic stellate cells in mouse. J Hepatol 2004;40:255–260.
12. Kisseleva T, Uchinami H, Feirt N, et al. Bone marrow-derived fibrocytes participate in pathogenesis of liver fibrosis. J Hepatol 2006;45:429–438.
13. Miyata E, Masuya M, Yoshida S, et al. Hematopoietic origin of hepatic stellate cells in the adult liver. Blood 2008;111:2427–2435.
14. Bou-Gharios G, Garrett LA, Rossert J, et al. A potent far-upstream enhancer in the mouse pro-α2(I) collagen gene regulates expression of reporter genes in transgenic mice. J Cell Biol 1996;134: 1333–1344.
15. De Val S, Ponticos M, Antoniv TT, et al. Identification of the key regions within the mouse pro-α2(I) collagen gene far-upstream enhancer. J Biol Chem 2002;277:9286–9292.
16. Okabe M, Ikawa M, Kominami K, et al. "Green mice" as a source of ubiquitous green cells. FEBS Lett 1997;407:313–319.
17. Inagaki Y, Kushida M, Higashi K, et al. Cell type-specific intervention of TGF-β/Smad signaling suppresses collagen gene expression and hepatic fibrosis in mice. Gastroenterology 2005;129: 259–268.
18. Kinoshita K, Iimuro Y, Fujimoto J, et al. Targeted and regulable expression of transgenes in hepatic stellate cells and myofibroblasts in culture and in vivo using an adenoviral Cre-LoxP system to antagonise hepatic fibrosis. Gut 2007;56:396–404.
19. Inagaki Y, Higashi K, Kushida M, et al. Hepatocyte growth factor suppresses profibrogenic signal transduction via nuclear export of Smad3 with galectin-7. Gastroenterology 2008;134:1180–1190.
20. Usuku T, Nishi M, Morimoto M, et al. Visualization of glucocorticoid receptor in the brain of green fluorescent protein-glucocorticoid receptor knock in mice. Neuroscience 2005;135: 1119–1128.
21. Inagaki Y, Truter S, Bou-Gharios G, et al. Activation of proα2(I) collagen promoter during hepatic fibrogenesis in transgenic mice. Biochem Biophys Res Commun 1998;250:606–611.
22. Thorgeirsson SS, Grisham JW. Hematopoietic cells as hepatocyte stem cells: a critical review of the evidence. Hepatology 2006;43:2–8.
23. Sakaida I, Terai S, Yamamoto N, et al. Transplantation of bone marrow cells reduces CCl_4-induced liver fibrosis in mice. Hepatology 2004;40:1304–1311.
24. Nakamura T, Torimura T, Sakamoto M, et al. Significance and therapeutic potential of endothelial progenitor cell transplantation in a cirrhotic liver rat model. Gastroenterology 2007;133: 91–107.
25. Asano Y, Iimuro Y, Son G, et al. Hepatocyte growth factor promotes remodeling of murine liver fibrosis, accelerating recruitment of bone marrow-derived cells into the liver. Hepatol Res 2007;37:1080–1094.
26. Direkze NC, Forbes SJ, Brittan FM, et al. Multiple organ engraftment by bone-marrow-derived myofibroblasts and fibroblasts in bone-marrow-transplanted mice. Stem Cells 2003;21:514–520.
27. Hashimoto N, Jin H, Liu T, et al. Bone marrow-derived progenitor cells in pulmonary fibrosis. J Clin Invest 2004;113:243–252.
28. van Amerongen MJ, Bou-Gharios G, Popa ER, et al. Bone marrow-derived myofibroblasts contribute functionally to scar formation after myocardial infarction. J Pathol 2008;214:377–386.
29. Kallis YN, Alison MR, Forbes SJ. Bone marrow stem cells and liver disease. Gut 2007;56:716–724.
30. Magness ST, Bataller R, Yang L, et al. A dual reporter gene transgenic mouse demonstrates heterogeneity in hepatic fibrogenic cell populations. Hepatology 2004;40:1151–1159.
31. McTaggart RA, Feng S. An uncomfortable silence while we all search for a better reporter gene in adult stem cell biology. Hepatology 2004;39:1143–1146.
32. Roufosse C, Bou-Gharios G, Prodromidi E, et al. Bone marrow-derived cells do not contribute significantly to collagen I synthesis in a murine model of renal fibrosis. J Am Soc Nephrol 2006;17: 775–782.

Received May 10, 2009. Accepted July 7, 2009.

Reprint requests

Address requests for reprints to: Yutaka Inagaki, MD, PhD, Professor, Research Unit for Tissue Remodeling and Regeneration, Tokai University School of Medicine, 143 Shimo-kasuya, Isehara, Kanagawa 259-1193, Japan. e-mail: yutakai@is.icc.u-tokai.ac.jp; fax: (81) 463-92-3549.

Acknowledgments

The authors thank Dr Benoit de Crombrugghe for his generous gift of transgenic collagen reporter mice, Dr Masaru Okabe for transgenic mice that constitutively express enhanced green fluorescent protein, and Dr Kiyoshi Higashi for his continuous support and helpful suggestions throughout the work.

Conflicts of interest

The authors disclose no conflicts.

Funding

Supported in part by a grant-in-aid from the Ministry of Education, Culture, Sports, Science and Technology, Japan; a grant from the Scleroderma Research Committee of the Ministry of Health, Labour and Welfare, Japan; and a research grant from Mitsui Life Social Welfare Foundation.

HUMAN GENE THERAPY 21:40–50 (January 2010)

DOI: 10.1089/hum.2009.027

In Vivo Stable Transduction of Humanized Liver Tissue in Chimeric Mice via High-Capacity Adenovirus–Lentivirus Hybrid Vector

Shuji Kubo,[1,2] Miho Kataoka,[3] Chise Tateno,[3] Katsutoshi Yoshizato,[3,4] Yoshiko Kawasaki,[2] Takahiro Kimura,[1] Emmanuelle Faure-Kumar,[1] Donna J. Palmer,[5] Philip Ng,[5] Haruki Okamura,[2] and Noriyuki Kasahara[1]

Abstract

We developed hybrid vectors employing high-capacity adenovirus as a first-stage carrier encoding all the components required for *in situ* production of a second-stage lentivirus, thereby achieving stable transgene expression in secondary target cells. Such vectors have never previously been tested in normal tissues, because of the scarcity of suitable *in vivo* systems permissive for second-stage lentivirus assembly. Here we employed a novel murine model in which endogenous liver tissue is extensively reconstituted with engrafted human hepatocytes, and successfully achieved stable transduction by the second-stage lentivirus produced *in situ* from first-stage adenovirus. This represents the first demonstration of the functionality of adenoviral-lentiviral hybrid vectors in a normal parenchymal organ *in vivo*.

Introduction

ADENOVIRAL VECTORS (AdVs) have been successfully used *in vivo* to transduce various postmitotic tissues, but generally only transient gene expression can be achieved because of cytotoxic T-lymphocyte–mediated immune responses against viral genes retained in conventional AdVs, and their extremely low frequency of chromosomal integration (Harui *et al.*, 1999; Wivel *et al.*, 1999). More persistent expression can be maintained by high-capacity, helper-dependent AdVs (HDAdVs) from which all of the viral coding sequences have been removed (Parks *et al.*, 1996; Schiedner *et al.*, 1998; Kochanek, 1999; Kim *et al.*, 2001; Oka *et al.*, 2001), but its duration is still limited because of progressive dilution of the extrachromosomal HDAdV vector DNA as transduced cells divide. Treatment of hereditary diseases may require more stable, long-term transgene expression, which can be achieved only through permanent integration or ongoing episomal replication of vector DNA.

To overcome this limitation, various hybrid vector systems have been developed, which employ AdV as a first-stage delivery vehicle to efficiently enter target cells, but then utilize the machinery of integrating viruses or mobile genetic elements to achieve permanent chromosomal integration (Feng *et al.*, 1997; Caplen *et al.*, 1999; Lieber *et al.*, 1999; Recchia *et al.*, 1999; Tan *et al.*, 1999; Leblois *et al.*, 2000; Soifer *et al.*, 2001; Soifer *et al.*, 2002; Yant *et al.*, 2002; Kubo and Mitani, 2003; Dorigo *et al.*, 2004; Picard-Maureau *et al.*, 2004). Efficient two-stage transduction *in vitro* and stable long-term transgene expression have previously been demonstrated with AdV–transposon (Soifer *et al.*, 2001; Yant *et al.*, 2002), AdV–adeno-associated virus (Lieber *et al.*, 1999; Recchia *et al.*, 1999), AdV–retrovirus (Feng *et al.*, 1997; Caplen *et al.*, 1999; Soifer *et al.*, 2002), AdV–foamy virus (Picard-Maureau *et al.*, 2004), and AdV–lentivirus (Kubo and Mitani, 2003) vectors. In particular, Kubo and Mitani (2003) have demonstrated the ability of an AdV–lentivirus hybrid vector to efficiently enter a variety of cell types via the first-stage HDAdV and subsequently mediate *in situ* production of a human immunodeficiency virus (HIV)-derived second-stage lentiviral vector (LV), which then stably delivers a marker gene to neighboring cells. However, this hybrid vector generated second-stage LV pseudotyped with the vesicular stomatitis virus G glycoprotein (VSV-G), a highly fusogenic and toxic envelope

[1]Division of Digestive Diseases, Department of Medicine, University of California at Los Angeles, Los Angeles, CA 90095.
[2]Laboratory of Host Defenses, Institute for Advanced Medical Sciences, Hyogo College of Medicine, Nishinomiya, Hyogo 663-8501, Japan.
[3]Yoshizato Project, CLUSTER, Hiroshima Prefectural Institute of Industrial Science and Technology, Higashi-Hiroshima, Hiroshima 739-0046, Japan.
[4]Developmental Biology Laboratory and Hiroshima University 21st Century COE Program for Advanced Radiation Casualty Medicine, Department of Biological Science, Graduate School of Science, Higashi-Hiroshima, Hiroshima 739-8526, Japan.
[5]Center for Cell & Gene Therapy, Baylor College of Medicine, Houston, TX 77030.

protein (Ory *et al.*, 1996), which may result in unwanted cytotoxic effects in the primary target cells during LV production. Further, the ability of AdV-lentivirus hybrid vectors to stably transduce normal quiescent tissues *in vivo* has never previously been tested.

We have now developed an improved high-capacity AdV-lentivirus hybrid vector system, designated HL, and examined the ability of this new hybrid system to mediate efficient and stable gene transfer *in vitro* and *in vivo*. The first-stage HDAdV of the HL hybrid system directs the production of a minimal second-stage LV that retains less than 800 bp of HIV sequence (Chen *et al.*, 2002) and is pseudotyped with the murine leukemia virus (MLV) 4070A amphotropic envelope, which is much less cytotoxic than VSV-G. However, to test the transduction efficiency of the new HL hybrid vector system, target cells that can support *in situ* production of the HIV-derived second-stage LV are required. For *in vitro* experiments, human cell lines permissive for HIV replication can be employed. However, the requirement for human target cells presents a challenge to testing the functionality of the HL hybrid vector system *in vivo*, particularly with respect to its ability to stably transduce normal organs and tissues.

As nearly 90% of the input dose of AdV introduced *in vivo* accumulates in the liver upon intravenous injection (Kass-Eisler *et al.*, 1994; Huard *et al.*, 1995; Kubo *et al.*, 1997), and nearly 100% transduction of hepatocytes can be achieved at higher doses (Li *et al.*, 1993), the liver is an attractive target for *in vivo* testing of the HL system. However, multiple blocks to HIV replication have been reported in rodent cells, including cellular entry, reduced abundance of unspliced HIV-RNA and *gag* proteins, and defects in infectious particle assembly (Hofmann *et al.*, 1999; Bieniasz and Cullen, 2000; Mariani *et al.*, 2000). Therefore, to test the HL hybrid vector *in vivo*, we sought a humanized liver model that is permissive for HIV particle assembly.

Successful reconstitution of human liver tissue has recently been achieved in immunodeficient mice (Dandri *et al.*, 2001; Mercer *et al.*, 2001). Dandri *et al.* (2001) reported that cross-breeding of recombinant activation gene-2–deleted mice with transgenic mice expressing the hepatotoxic urokinase-type plasminogen activator (uPA) results in immunodeficient progeny which undergo progressive liver degeneration. These progeny were successfully transplanted with human hepatocytes, resulting in chimeric liver tissue with a replacement index of up to 15%, rendering these mice permissive for HBV infection (Dandri *et al.*, 2001). Similarly, Mercer *et al.* (2001) demonstrated that uPA/SCID mice bearing chimeric humanized livers with replacement index values of 50% could support HCV replication (Dandri *et al.*, 2001). More extensive repopulation has been difficult to achieve, likely because engrafted human hepatocytes produce complement factors, which appear to exert lethal effects in mice with higher replacement values. However, Tateno *et al.* (2004) and Yoshizato and colleagues (2004) have recently demonstrated that administration of a C5/C3 convertase inhibitor successfully rescued uPA/SCID mice whose chimeric livers proved to be almost completely repopulated with human hepatocytes exhibiting normal cytoarchitecture. The transduction efficiency of oncoretroviral vectors has previously been tested in this humanized liver model, and consistent with their inability to enter quiescent postmitotic cells, was found to be in the order of 5% (Emoto *et al.*, 2005). We have now utilized this unique chimeric liver model to test the ability of the HL hybrid system to mediate efficient entry by the first-stage HDAdV, *in situ* production of the second-stage LV, and stable transduction in fully humanized livers *in vivo*. To our knowledge, this represents the first report of *in vivo* testing of an AdV–lentivirus hybrid vector system in a normal parenchymal organ.

Materials and Methods

Cells

Cell lines including 293 (Graham *et al.*, 1977) (Microbix, Toronto, Canada), 293T (DuBridge *et al.*, 1987), and the Gli36 human glioma (Sena-Esteves *et al.*, 2000) were cultured in Dulbecco's modified Eagle's medium supplemented with 10% fetal calf serum (FCS; Omega, Tarzana, CA). Hep3B human hepatocellular carcinoma cells were cultured in Eagle's minimum essential medium supplemented with 10% FCS, 1 m*M* sodium pyruvate, and nonessential amino acids. Primary human hepatocytes and their specific medium were purchased from Cambrex (Baltimore, MD; CC-2591).

HL first-stage HDAdV construction and production

The phosphoglycerokinase promoter-driven green fluorescence protein (GFP) marker gene cassette, cytomegalovirus promoter (CMV)-driven *gag/pol/rev* lentiviral packaging cassette, simian virus 40 early promoter-driven MLV 4070A amphotropic envelope cassette, and minimal LV construct (Robbins *et al.*, 1998; Chen *et al.*, 2002) were sequentially cloned into the HDAdV plasmid pSTK120, which contains the human Ad5 inverted terminal repeat sequences and packaging signal, resulting in the construction of the complete HL vector plasmid, pHL. Additional details regarding the pHL construct, and the HIV-based minimal LV contained therein, are provided upon request.

The HL vector and control HDAdV cmv-GFP (Ad GFP) were prepared using the FLPe/*FRT* helper virus system (Umana *et al.*, 2001). The vectors were titrated on 293 cells for GFP expression, using a FACScalibur flow cytometer (Becton Dickinson, San Jose, CA), on day 2 post-infection, defined as transducing units per ml (TU/ml). Another control HDAdV, HDΔ28E4LacZ, was prepared as previously described (Palmer and Ng, 2003). Helper virus contamination levels were determined by Southern blot, as previously described (Kubo and Mitani, 2003).

Second-stage LV production after infection with HL first-stage HDAdV

To confirm production of LV in cells (Gli36, HeLa, Hep3B, HepG2 and human primary hepatocytes) infected by the HL vector, 4×10^5 cells of each were infected with various amounts of HL vector. The amount of vector used for each infection was based on the titer determined using each cell line. At 4 hr postinfection, the infected cells were washed three times with phosphate-buffered saline (PBS), and incubated in growth medium. At 48 hr postinfection, the virus-containing medium was harvested, centrifuged, filtered through a 0.45-μm pore filter, and used for titration on 293 cells by X-galactosidase (gal) staining to detect βgal expression. In preliminary experiments, the level of residual adenovirus carried over in the filtered supernatant medium after infection of primary cells at a multiplicity of infection (MOI) of 10, as

measured by flow cytometry for GFP expression in secondary cells, was less than 1%.

To inhibit lentiviral infection, 293 cells were infected with the viral supernatant in the presence or absence of 5 μM zidovudine (AZT; Sigma, St. Louis, MO).

To investigate the kinetics of LV vector production after HL vector infection, 4×10^5 Hep3B cells were infected with HL at various MOIs in six-well plates. The medium was collected at different time points and titrated on 293 cells, as described earlier.

Long-term culture experiments

Hep3B cells (2×10^5) were infected with the HL vector, at an MOI of 10, and incubated in the presence of AZT on a 10-cm dish. The cells were split at a ratio of 1:20 once a week, and expression of GFP was examined by flow cytometry. At each passage, DNA was extracted from a portion of the cells and analyzed for proviral integration by Southern hybridization. A part of the HL-infected cells were also plated on Lab-Tek chamber slides (Thermo Fisher Scientific, Rochester, NY). The next day, the cells were fixed for 10 min with 4% paraformaldehyde, washed with PBS, and incubated with 50 mM NH_4Cl in PBS for 5 min. The cells were permeabilized in 0.5% Triton/PBS for 5 min and then incubated for 30 min in 1% bovine serum albumin/PBS for blocking. The cells were incubated for 1 hr with a 1:1000 dilution of mouse anti-GFP monoclonal (Chemicon, Temecula, CA). Immunoreactivity for GFP was visualized with a 1:5000 dilution of goat anti-mouse immunoglobulin G (IgG) (H + L) Alexa Fluor 488. The cells were then incubated with a 1:1000 dilution of rabbit anti-βgal polyclonal (ab616; Abcam, Cambridge, MA). Immunoreactivities for βgal were visualized with a 1:5000 dilution of goat anti-rabbit IgG (H + L) Alexa Fluor 594 (Molecular Probes, Eugene, OR).

Animals

Chimeric mice with human liver were generated as previously described (Tateno *et al.*, 2004). Briefly, uPA/SCID mice were generated by crossing uPA mice [B6SJL-TgN(Alb1Plau)144Bri; The Jackson Laboratory, Bar Harbor, ME] with SCID mice (Fox Chase SCID C.B-17/Icr-*scid* Jcl; Clea Japan, Tokyo, Japan). The $uPA^{+/+}SCID^{+/+}$ mice were screened by polymerase chain reaction (PCR) and injected with $5.0–7.5\times10^5$ viable human hepatocytes (IVT079; In Vitro Technologies Inc., Baltimore, MD) through a small left-flank incision into the inferior splenic pole at 20–30 days after birth. The mice were injected intraperitoneally with 200 μl of 1.5 mg/ml Futhan (nafamostat mesilate, 6-amidino-2-naphthyl *p*-guanidinobenzoate dimethanesulfonate; gift from Torii Pharmaceutical, Tokyo, Japan) to enhance repopulation of the liver with human hepatocytes. The replacement index was estimated by serum level of human albumin as previously described (Tateno *et al.*, 2004). Generally, >5 mg/ml human albumin in the blood indicates high replacement index values of >70%, and mice screened in this manner were used for experiments at 6–8 weeks posttransplantation.

After injection with gadolinium (10 mg/kg body weight) to eliminate Kupffer cells (Lieber *et al.*, 1997), either HL vector (2×10^9 TU/200 ml) or buffer (PBS) was injected via tail vein, followed by sacrifice at 4 days or 4 weeks postinfection ($n = 4$ per group). A portion of each liver sample was immediately digested into cell suspensions and used for flow cytometric analysis. The remaining portion was frozen in liquid nitrogen for isolation of genomic DNA or for frozen tissue sections. Immunofluorescence (IF) and immunohistochemistry (IHC) for GFP were performed on frozen liver sections using standard methods with GFP-specific antibodies (ab290; Abcam): goat anti-rabbit IgG-Alexa Fluor 488 for IF, or Vectastain ABC kit (Vector Laboratories, Burlingame, CA) and diaminobenzidine for IHC. IF for βgal was also performed using rabbit anti-βgal antibodies (ab616; Abcam) and goat anti-rabbit IgG-Alexa Fluor 594, as earlier. X-gal staining using standard methods was also performed on glutaraldehyde-fixed liver sections, and the proportion of βgal-positive cells was determined by image analysis using the SPOT digital imaging system and NIH ImageJ software (version 1.34). The replacement index of the mouse liver with human hepatocytes was also determined by IHC for human-specific cytokeratin-8 and -18 (CK8/18) as previously described (Tateno *et al.*, 2004) and is defined as the ratio of area occupied by human hepatocytes to the entire area examined. To assess any potential hepatotoxicity, sera were collected from mice at the time of scheduled sacrifice, that is, at 4 weeks after injection with HL vector or PBS, and serum levels of aspartate amino transferase (AST) were measured by automated colorimetric assay.

Molecular analysis of integrated LVs in the liver

High-molecular-weight genomic DNA was extracted from livers injected with HL vector or PBS. For detection of the stably integrated form of the second-stage LV after production from the first-stage HDAdV, high-molecular-weight genomic DNA (500 ng) was subjected to nested PCR to amplify lentiviral integration events close to or within *Alu* repeat sequences in the human genome (Nguyen *et al.*, 2002; Serafini *et al.*, 2004). Briefly, the first PCR (PCR1) was carried out using a sense oligomer specific for the conserved sequences of human *Alu* (*Alu*-s; 5′-TCCCAGCTACTCGGGA GGCTGAGG-3′) and an antisense oligomer specific for the PBS region of HIV-1 upstream of *gag* (5NC2-as; 5′-GAGTC CTGCGTCGAGAGAG-3′). All amplifications were done using 100 μl of reaction mixture containing 200 ng of genomic DNA, 0.4 mM of each dNTP, 0.8 μM of each sense and antisense primer, 5% dimethyl sulfoxide, and 2 U *Taq* DNA polymerase. After the first DNA denaturation at 95°C for 5 min, 30 amplification cycles were performed consisting of denaturation for 1 min at 94°C, annealing for 1 min at 60°C, and extension for 3 min at 72°C. One aliquot (1:100 dilution) of the first PCR products was subjected to a second PCR (PCR2) amplification using the nested primers, LTR9-s (5′-GCCTCAATAAAGCTTGCCTTG-3′) and U5PBS-as (spanning the U5LTR/PBS boundary region) (5′-GGCGCCAC TGCTAGAGATTTT-3′), which amplified a fragment of 121 bp. The nested PCR conditions were similar to those of the first amplification, except for an annealing temperature of 55°C and an extension time of 1 min. Twenty amplification cycles were performed. In control reactions, genomic DNA that had not been subjected to the first round of PCR was also amplified using the second PCR primers to exclude the presence of residual nonintegrated vector DNA. As a loading control, the same DNA samples were subjected to a PCR that amplified a 610-bp region of human β-actin (5′-GATCAT GTTTGAGACCTTCA-3′ and the reverse sequence 5′-ACC

TTGATCTTCATGGTGC-3′), with the following amplification conditions: 95°C for 2 min, then 30 cycles of 95°C for 30 sec, 65°C for 30 sec, and 72°C for 1 min, followed by a final extension at 72°C for 5 min. Amplification products were resolved on 1.5% agarose gel containing ethidium bromide and detected by ultraviolet transillumination.

The copy number of the integrated form of the lentiviral construct in each cell was determined by quantitative real-time PCR (Q-PCR) with βgal-specific primers and probe, designed using Primer Express software V. 1.0 (Applied Biosystems, Foster City, CA). Primer and probe sequences spanned a 91-bp region in the βgal-coding region, consisting of the following sequences: forward primer, 5′-CTATCCC GACCGCCTTACTG-3′; reverse primer, 5′-GTTTTCGCTCG GGAAGACGTA-3′; probe, 5′-FAM-CAGCGGTCAAAA CAG-TAMRA-3′. Amplification was performed in a reaction volume of 25 μl under the following conditions: 300 ng of high-molecular-weight genomic DNA, 1×Taqman universal PCR master mix (Applied Biosystems), 600 n*M* forward primer, 900 n*M* reverse primer, and 100 n*M* probe. Thermal cycling conditions were 2 min incubation at 50°C, 10 min at 95°C, followed by 40 cycles of successive incubation at 95°C for 15 sec and 60°C for 1 min. Standard curves were generated using serial dilutions of HL vector plasmid, pHL, from 5 to 50,000,000 copies in a background of 50,000 equivalents (300 ng) of untransduced genomic DNA from the chimeric mouse liver. Duplicate samples were amplified in an ABI Prism 7700 sequence detector with continuous fluorescence monitoring. Data were collected and analyzed using 7700 Sequence Detection System software v.1.6.3. (Applied Biosystems). The copy number per cell of integrated lentiviral construct was calculated as the average copy number divided by 50,000 cells (equivalent to 300 ng genomic DNA).

Statistical analysis

The results are presented as mean ± standard deviation. Statistical significance of differences was calculated using Student's *t*-test, and a *p*-value of <0.01 was considered significant.

Results

Design and production of the HL hybrid vector

The hybrid vector HL contains a complete set of HIV-derived lentiviral packaging components incorporated into an HDAdV (Fig. 1A), including (1) a multiple attenuated packaging construct expressing *gag-pol, rev,* and the *rev* response element sequence, (2) an envelope construct expressing amphotropic (i.e., broad mammalian host range) *env* from MLV strain 4070A, and (3) a minimal HIV-based LV transfer vector encoding a βgal marker gene driven by a methylation-resistant MLV promoter (MND promoter) (Chen *et al.*, 2002). As this transfer vector sequence contains a LV packaging signal so that its mRNA will be encapsidated by the coexpressed packaging and envelope components to form LV virions, the βgal transgene will not only be expressed in cells directly infected by the HDAdV, but also be transmitted to adjacent cells. The adenoviral backbone

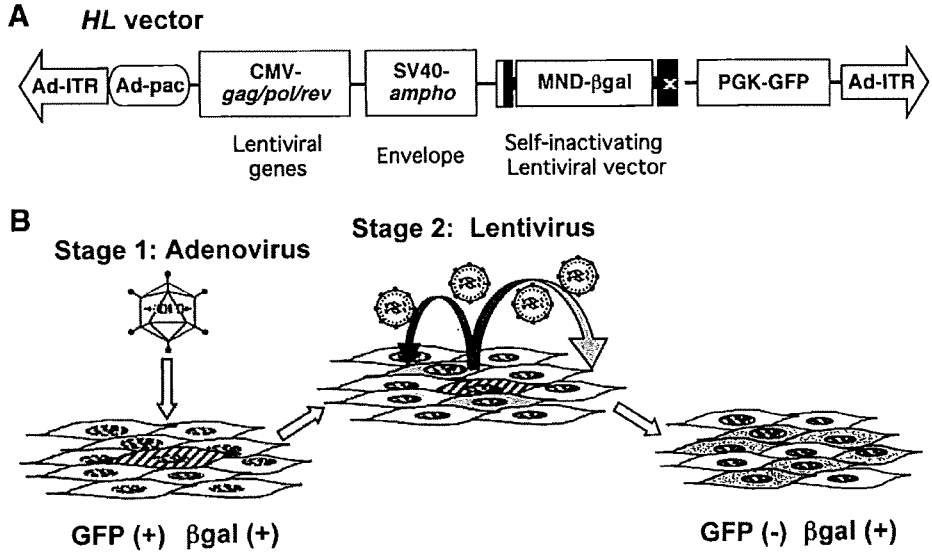

FIG. 1. Outline of the high-capacity adenovirus/lentivirus hybrid vector (HL vector) system. (**A**) Schematic structure of the HL vector. An HL vector is a helper-dependent adenoviral vector encoding expression cassettes for production of a lentiviral vector (LV) based on human immunodeficiency virus 1 (HIV-1). The HL vector has two inverted terminal repeats (Ad-ITR) and the packaging signal (Ad-pac) of human adenovirus type 5 and encodes four gene expression cassettes: (1) a self-inactivating minimal LV that contains the central polypurine tract, the woodchuck hepatitis virus posttranscriptional regulatory element, and the β-galactosidase gene (βgal) driven by the methylation-resistant murine leukemia virus LTR promoter (MND) (Robbins *et al.*, 1998; Chen *et al.*, 2002) as a marker; (2) HIV-*gag/pol/rev* coding sequences driven by cytomegalovirus (CMV) promoter; (3) the amphotropic murine leukemia virus envelope driven by the simian virus 40 early promoter (SV40) for pseudotyping of the lentivirus; and (4) the enhanced green fluorescent protein (GFP) driven by phosphoglycerokinase (PGK) promoter as a marker of the adenoviral backbone. (**B**) Two-stage transduction with the HL vector. The HL vector infects the initial target cells efficiently as an adenoviral vector and produces an LV *in situ*. The LV then infects surrounding secondary target cells and integrates into chromosomes for stable gene expression.

sequence also contains a GFP expression cassette unlinked to the LV components; the GFP marker gene will not be encapsidated into LV particles, thereby allowing specific quantitation of initial transduction by HDAdV itself. Thus, it is possible to distinguish between untransduced cells [GFP (−), βgal(−)], cells transduced by HL first-stage HDAdV only [GFP(+), βgal(+)], and cells transduced by HL second-stage LV [GFP(−), βgal(+)] (Fig. 1B).

The first-stage HDAdV was propagated using the FRT/FLPe helper system (Umana *et al.*, 2001). The GFP titers of purified HL vector preparations on 293 cells ranged from 4.1×10^9 to 1.8×10^{10} TU/ml. Vector stocks contained less than 0.1% helper virus contamination, as determined by Southern hybridization, using a probe for the adenoviral packaging signal (data not shown).

Infection with HL first-stage HDAdV results in production of functional second-stage LV

Following infection by the HL first-stage HDAdV vector at various MOIs, cell-free conditioned media from various human cell lines, including Gli36 (glioma), HeLa (cervical adenocarcinoma), and Hep3B and HepG2 (both hepatocellular carcinoma), were inoculated into fresh 293 cell cultures and tested for their ability to mediate secondary transmission of βgal expression. For all primary target cell lines tested, increasing MOI during first-stage HDAdV transduction correlated with increasing βgal transmission to secondary target cells (Fig. 2A). Further, βgal expression in secondary target cells was markedly suppressed by the reverse transcriptase inhibitor AZT, indicating that the observed transmission was indeed mediated by second-stage LV and was not due to carry-over of the first-stage HDAdV or pseudotransduction by overexpressed βgal protein (Fig. 2B). Of the cell lines tested, Gli36 and Hep3B produced the highest titers of LV (1.0×10^4 and 5.1×10^4 TU/ml, respectively, at MOI = 100) (Fig. 2A), which also correlated with high levels of p24 production (236 and 316 ng/ml, respectively). Primary human hepatocytes also produced LV at titers of 6.0×10^1, 1.0×10^3, and 1.2×10^4 TU/ml upon infection with 1, 10, and 100 μl of HL vector (4.0×10^8 TU/ml), respectively. Taken together, these findings indicate that the HL hybrid vector is

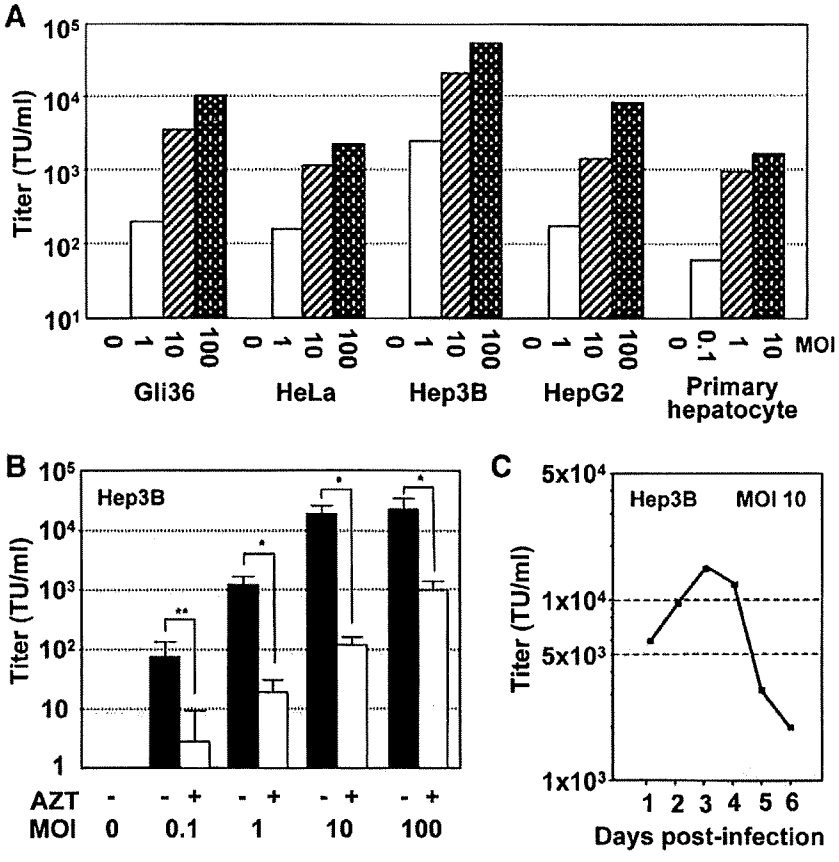

FIG. 2. Production of LV via HL vector system. (A) Production of LV in a variety of cell types after HL infection. Various cell lines indicated in the figure were infected with HL at multiplicity of infections (MOIs) of 1, 10, or 100. After 48 hr, viral supernatant was collected and titrated on 293 cells for βgal expression. (B) Production of LV following HL vector infection. Hep3B cells were infected with the HL vector at MOIs of 0.1, 1, 10, or 100. After 48 hr, viral supernatant was collected and titrated on 293 cells for βgal expression in the presence or absence of zidovudine (AZT, 5 μM). Data shown are average titers and standard deviations from the experiment performed in triplicate. Effect of AZT on titers was determined by Student's *t*-test (**$p < 0.05$, *$p < 0.01$). (C) Time course of lentiviral production from Hep3B cells infected with the HL vector. Hep3B cells were infected with HL at an MOI of 10 and monitored for up to 6 days. At different time points indicated in the figure, the medium was replaced, and the viral supernatant was titrated for βgal expression on 293 cells.

capable of directing the production of infectious LV particles from a variety of cell types, and that the LV yield is dependent upon the MOI and the target cell type.

To determine how long cells can produce LV after being infected with the HL first-stage HDAdV vector, a time-course experiment was performed. After infection of Hep3B cells with the HL first-stage HDAdV vector at an MOI of 10, the culture medium was harvested and replaced with fresh medium every day. The LV titers of the conditioned media harvested daily were measured on secondary target cells and were found to increase, reaching a peak level by day 3 post-HDAdV infection (1.3×10^4 TU/ml; Fig. 2C). Thereafter, HL-infected human cells continued to sustain LV production for several days (postinfection day 6 titer = 2.0×10^3 TU/ml).

In vitro *persistence of second-stage LV-transduced cells following HL first-stage HDAdV infection*

The spread of lentivirus in long-term cultures of HL-infected cells was examined by maintaining infected Hep3B in culture (Fig. 3A). As expected, GFP expression from the adenovirus backbone significantly decreased over time because of ongoing cell division-mediated dilution of HDAdV episomes in the culture. The percentage of GFP-positive cells

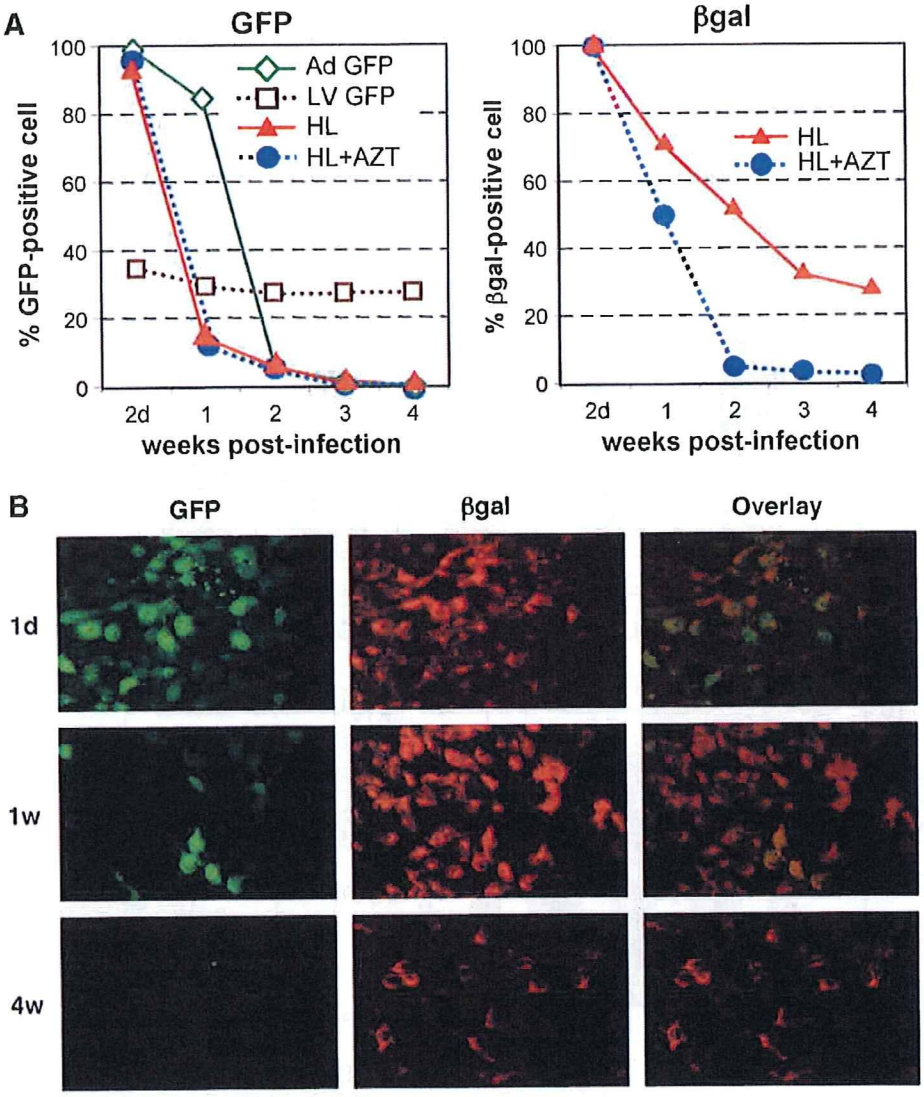

FIG. 3. Spread of LV-transduced cells and persistent gene expression following HL vector infection. (**A**) Transduction efficiencies of HL hybrid vector-infected cells. Hep3B cells (2×10^5) infected with the HL vector at an MOI of 10 were incubated overnight, and the cells were split the following day and cultivated in the presence (blue circle) or absence (red triangle) of AZT on a 10-cm dish. The control samples infected with an LV GFP (brown square) or an Ad GFP (green diamond) are also shown. The cells were passaged at a ratio of 1:20 every week, and expressions of GFP and βgal were examined. Data are representative of three independent experiments, all yielding similar results. (**B**) Persistent gene expression achieved via HL hybrid vector system in transformed human hepatocytes *in vitro*. Hep3B cells were infected with HL vector at an MOI of 10. The cells were passaged at a ratio of 1:20 every week. Expressions of GFP and βgal were analyzed by immunofluorescence staining using anti-GFP and anti-βgal antibody at the indicated time points after HL infection.

quickly decreased from >90% to <2% within 2 weeks postinfection in the HL-infected cells (HL and HL + AZT) as well as in cells infected with control Ad GFP. Initially, a parallel decrease in βgal-positive cells was observed. However, 25% of the HL-infected cells (HL) remained βgal positive at 4 weeks postinfection, whereas those in the HL-infected/AZT-treated cells (HL + AZT) were <2% βgal positive within 2 weeks postinfection. Persistent βgal expression in the HL-infected cells (HL) was also confirmed by IF staining (Fig. 3B). Southern hybridization of high-molecular-weight genomic DNA extracted from the cells at week 4 confirmed LV proviral integration and a direct correlation between βgal expression and the copy number of the integrated βgal transgenes (data not shown). This also demonstrates that persistent βgal expression in the HL-infected cells is mediated by stable transduction with the HL second-stage LV vector.

In vivo *persistence of second-stage LV-transduced cells in humanized liver following intravenous administration of HL first-stage HDAdV*

In vivo testing of the HL vector system requires a model that is permissive for assembly of human lentivirus. We employed a unique humanized model in which endogenous murine hepatocytes are extensively replaced with human hepatocytes. The replacement indices, calculated as the frequency of human-specific CK8/18-positive regions relative to that of the entire examined area in the mouse liver (Tateno *et al.*, 2004), ranged from 63.7% to 86.6% (Fig. 4A). This model was found to be efficiently transduced by control HDAdV (HDΔ28E4LacZ) (Palmer and Ng, 2003) (data not shown), and so chimeric uPA/SCID mice with highly humanized livers were intravenously injected with the HL first-stage HDAdV vector.

First, GFP expression from the adenoviral backbone of the HL first-stage HDAdV in liver tissue was analyzed by flow cytometry. The results showed 7.64% ± 1.33% GFP-positive cells at 4 days postinfection and 0.21% ± 0.07% GFP-positive cells at 4 weeks postinfection. This reduction in GFP-positive hepatocytes was also confirmed by IF (Fig. 4B) and IHC (Fig. 4C).

On the other hand, βgal expression persisted for at least 4 weeks postinfection as shown by IF studies (Fig. 4D) and X-gal tissue staining (Fig. 4E). Quantitation by image analysis revealed that the percentage of βgal-positive cells increased from 16.21% ± 3.70% at 4 days, to 28.40 ± 4.92% at 4 weeks postinfection ($p = 0.0074$). The persistence of βgal expression suggested that stable integration by the second-stage LV might have occurred. To demonstrate integration of second-stage LV in human hepatocyte genomic DNA *in vivo*, nested *Alu*–lentivirus PCR was performed (Nguyen *et al.*, 2002; Serafini *et al.*, 2004). In this assay, the first round of PCR was performed using a sense primer specific for human *Alu* sequences and another primer specific for the lentiviral 5′ noncoding region as the antisense primer (*Alu*-s and 5NC2-as, respectively; Fig. 5A). As LV vectors randomly integrate at multiple sites and repetitive *Alu* sequences are scattered throughout the human genome, the first reaction generated products with variable sizes (Fig. 5B, PCR1). The second round of PCR, using nested primers within the viral LTR and the viral primer binding site, respectively ("LTR9-s" sense and "U5 PBS-as" antisense primers, as depicted in Fig. 5A), generated the expected 140-bp product from transduced liver tissues, but not from untransduced control liver (Fig. 5B, PCR1 + PCR2). Genomic DNA from transduced cells subjected only to second-round PCR amplification did not yield any signal, validating the inability of the nested primers alone to amplify any residual episomal LV sequences and confirming the requirement for first-round amplification with the *Alu*–lentivirus primers to detect integrated proviruses (Fig. 5B, PCR2). Although this is not a quantitative assay, taken together these results do demonstrate integration of the lentiviral sequences into the genome of human hepatocytes *in vivo*.

For further quantitative assessment of the percentage of cells expressing βgal from the lentivirus vector component, Q-PCR was again performed, this time using high-molecular-weight genomic DNA from each of liver tissues as the template and with primers and probe specific for the βgal gene. The Q-PCR results demonstrated that the percentage of βgal-positive cells was 13.8–56.6% at 4 weeks postinfection, correlating with the data obtained by Xgal staining (28.40% ± 4.92%) (Fig. 4E). These results indicate that *in situ* production and spread of second-stage LV had occurred in the humanized livers of chimeric mice following systemic administration of the HL first-stage HDAdV, and taken together with the above finding that the first-stage HDAdV was undetectable at 4 weeks postinfection, it is likely that βgal expression at a later time point is derived almost entirely from the second-stage LV.

To assess any potential vector-related hepatotoxicity, serum AST levels were measured and compared between HL vector-injected and control PBS-injected mice. It should be noted that the levels of serum liver enzymes in the uPA/SICD-based chimeric mouse model are generally high because of the ongoing hepatic expression of uPA, which mediates progressive destruction of murine hepatocytes and thereby allows gradual engraftment of human hepatocytes. Notably, however, there was no significant difference in the serum AST levels between HL-injected mice (272.5 ± 154.5 U/l) and PBS-treated group (453.0 ± 79.3 U/l) ($p = 0.1546$). Consistent with these findings, liver histology showed no significant difference between PBS- and HL vector-treated livers. Taken together with the serum AST levels, this indicates that the HL vector does not cause significant liver toxicity. In addition, as noted earlier, serum levels of human albumin remained at high values (>5 mg/ml) throughout these experiments, and replacement indices remained at high levels, ranging from 63.7% to 86.6% (Fig. 4A), further indicating that the HL vector does not show any selective toxicity that would alter the proportion of human hepatocytes.

Discussion

The liver has a variety of characteristics that make it a significant target for gene therapy (Ferry and Heard, 1998). As the liver is the site of essential metabolic pathways, it is involved in many inborn metabolic diseases. Moreover, because of its highly vascularized architecture and position as a portal to blood circulation, the liver can serve as a secretory organ for the systemic delivery of therapeutic proteins. Because of the fenestrated structure of its endothelium, the liver parenchyma is readily accessible to large molecules such as DNA or recombinant viruses via the blood stream. AdVs accumulate

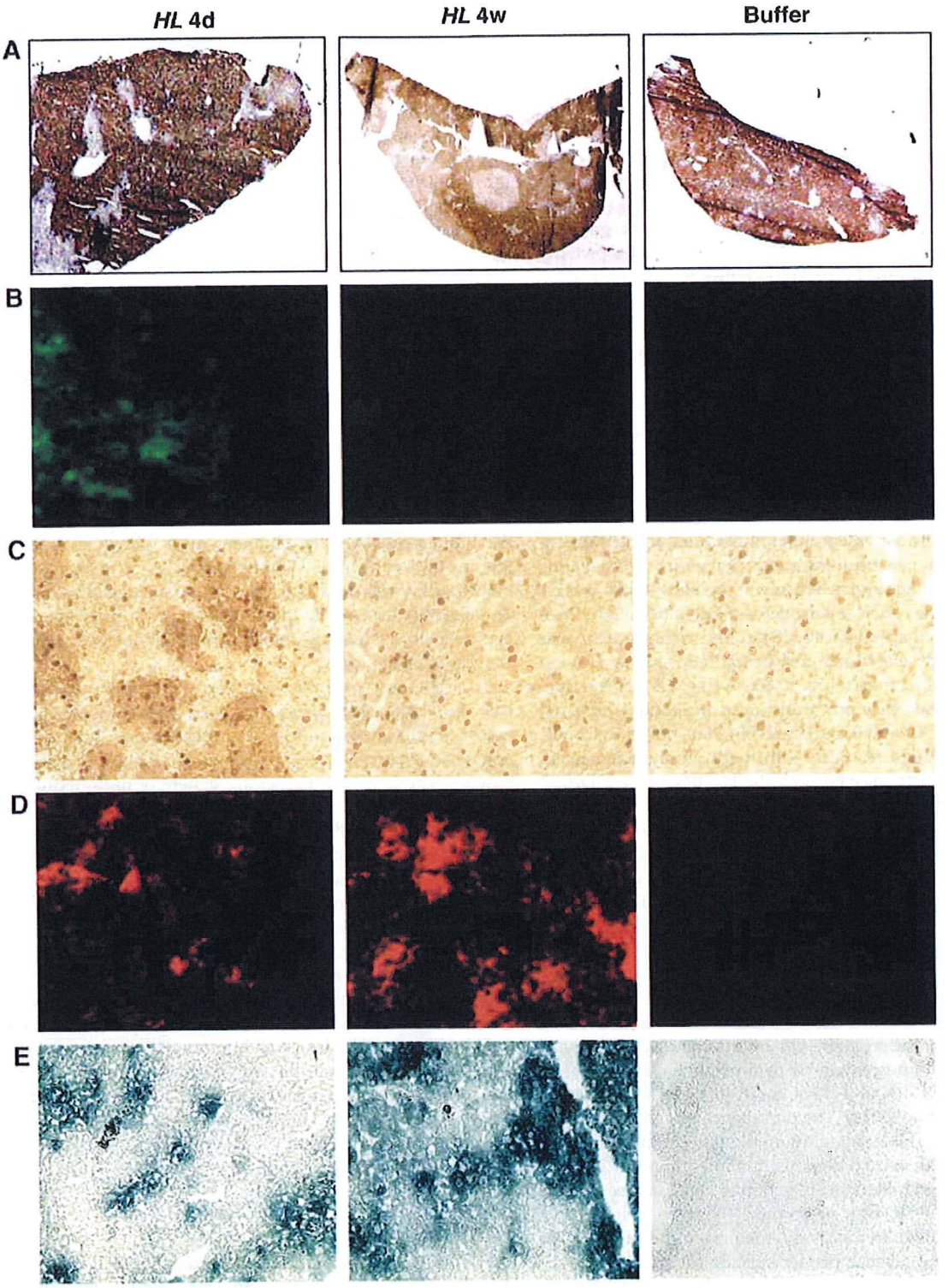

FIG. 4. *In vivo* transduction in humanized liver of the chimeric mice via HL hybrid vector system. The mice were injected with HL vector or phosphate-buffered saline (PBS) buffer. At indicated time points following HL infection, liver tissue was analyzed for GFP and βgal expression as follows: (**A**) Human CK8/18 immunostaining to determine replacement index of the mouse liver with human hepatocytes (human hepatocytes appear brown). Original magnification: 10×. (**B**) Immunofluorescence stain for GFP. Original magnification: 200×. (**C**) Immunohistochemical stain for GFP. Original magnification: 200×. (**D**) Immunofluorescence staining for βgal. Original magnification:×200. (**E**) X-gal staining. Original magnification:×100. Representative sections of each stain are shown.

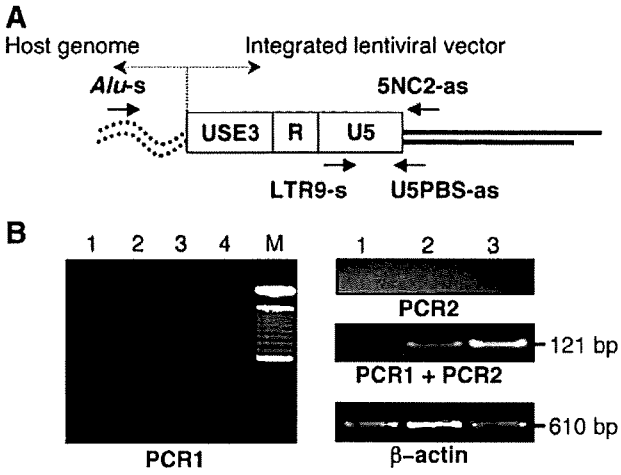

FIG. 5. Detection of integrated second-stage LV in liver tissue from chimeric mice after HL vector administration. (**A**) Design of nested polymerase chain reaction (PCR) analysis to amplify sequences spanning adjacent *Alu* repeats in the human genome (*Alu*-s and 5NC2-as) and the integrated lentiviral LTR (LTR9-s and U5PBS-as) (Nguyen *et al.*, 2002; Serafini *et al.*, 2004). (**B**) Result of nested PCR analysis: PCR1 and PCR2 correspond to the first and second rounds of nested PCR, respectively. M, 1-kb molecular mass size ladder (Invitrogen); lane 1, PBS-treated; lane 2, HL-infected, 4 days postinfection; lane 3, HL-infected, 4 weeks postinfection; lane 4, no DNA template. The 121-bp final amplification product is indicated. A 500-bp region of the human β-actin gene was amplified from the same samples as an internal control.

in the liver when injected intravenously (Kass-Eisler *et al.*, 1994; Huard *et al.*, 1995; Kubo *et al.*, 1997) and can achieve efficient hepatic gene delivery *in vivo* (Li *et al.*, 1993). The newer HDAdV system evades immune responses against transduced cells, thereby achieving long-term expression in the liver (Kim *et al.*, 2001; Oka *et al.*, 2001). However, HDAdV vectors still cannot overcome the limited duration of expression due to dilution of viral DNA as cells start to divide, a situation exacerbated if corrected hepatocytes have a selective growth advantage (Overturf *et al.*, 1996; De Vree *et al.*, 2000). Thus, the use of integrating vectors such as oncoretroviruses and lentiviruses has also been pursued.

However, hepatocytes are usually arrested in the G_0 phase of the cell cycle (Ferry and Heard, 1998), and the *in vivo* transduction efficiency of oncoretrovirus vectors is extremely low unless cell division is stimulated by growth factors or partial hepatectomy (Bosch *et al.*, 1996; Patijn *et al.*, 1998). In fact, the transduction efficiency of oncoretroviral vectors in the present uPA/SCID humanized liver model is only about 5% (Emoto *et al.*, 2005). Even though cellular mitosis is not absolutely required for lentiviral transduction, it has been reported that hepatocytes may be refractory even to lentiviral transduction unless they progress into the cell cycle (Park *et al.*, 2000), and certainly lentiviruses are incapable of efficiently transducing cells in G_0 phase, presumably because of lack of sufficient free nucleotide pools to support reverse transcription (Naldini *et al.*, 1996; Korin and Zack, 1998). As AdVs can readily infect nondividing cells (Benihoud *et al.*, 1999), it is quite advantageous to employ HDAdV as an efficient first-stage delivery vehicle for initial transient transduction of hepatocytes *in vivo*.

As the uPA/SCID chimeric mice are immunodeficient (Tateno *et al.*, 2004) and our hybrid vector is based on the HDAdV system which itself exhibits low immunogenicity (Kim *et al.*, 2001; Oka *et al.*, 2001), it might be anticipated that the HDAdV vector backbone would persist for an extended period of time in the engrafted human hepatocytes. Instead, expression of GFP in the humanized livers decreased significantly within 4 weeks after HL infection. It is possible that the toxic effects of HL-derived protein products (HIV-associated proteins and marker gene products) in the transduced cells might contribute to the activation of cell cycling in the liver; however, serum AST levels and liver histology of vector-injected animals were not significantly different from those of controls. In any case, loss of the HL-adenoviral episome would actually be advantageous to shutdown further production of the second-stage LV. To increase safety, a regulatable expression system could also be introduced into the hybrid vector to regulate LV production as reported previously (Kubo and Mitani, 2003).

Second-stage LV production *in situ* following HL vector-mediated hepatic gene transfer was assessed *in vivo* using chimeric mice in which the replacement indices indicated that the livers were almost completely repopulated with human hepatocytes. These chimeric mice have previously been shown to be a useful model for assessing the functions and pharmacological responses of human hepatocytes (Tateno *et al.*, 2004), but had never been previously employed in the evaluation of gene transfer efficiency with viral vectors.

In this humanized liver model, we observed persistent βgal expression associated with detection of integrated lentivirus sequences, despite a progressive decrease in GFP expression, suggesting that successful *in situ* production of LV had been achieved in HL-infected human hepatocytes. As noted earlier, stimulation of hepatocellular cycling after first-stage HDAdV infection might have accelerated the loss of adenoviral episomes, but may also have helped to enhance second-stage LV-mediated transduction of adjacent cells. As endogenous expression of the amphotropic envelope generally results in sequestration of the viral receptor and resistance to superinfection, it seems unlikely that cells initially transduced by the first-stage HDAdV would be reinfected with the second-stage LV. Genomic integration of the second-stage lentivirus vector was confirmed by PCR using human *Alu* and HIV LTR-specific primers. These data provide proof-of-principle for the use of the HL hybrid vector system to transduce liver parenchyma *in vivo* and for the use of the uPA/SCID mice as a model for gene delivery to human hepatocytes.

Acknowledgments

The authors thank Pedro Lowenstein for providing the FLP recombinase-based HDAdV helper system; Luigi Naldini and Didier Trono for the lentiviral packaging constructs; Stefan Kochanek for the STK plasmid; Paula Cannon for the minimal lentiviral vector; Chimoto Ohnishi for flow cytometric analysis; Maria Barcova, Celina Ngiam, and Ruth Margalit for their help during the preliminary phase of this work; and Karin Gaensler for helpful discussion. This work was supported by an NIH grant R01 CA93709 (to N.K.).

Disclosure Statement

No competing financial interests exist.

References

Benihoud, K., Yeh, P., and Perricaudet, M. (1999). Adenovirus vectors for gene delivery. Curr. Opin. Biotechnol. 10, 440–447.

Bieniasz, P.D., and Cullen, B.R. (2000). Multiple blocks to human immunodeficiency virus type 1 replication in rodent cells. J. Virol. 74, 9868–9877.

Bosch, A., McCray, P.B., Jr., Chang, S.M., Ulich, T.R., Simonet, W.S., Jolly, D.J., and Davidson, B.L. (1996). Proliferation induced by keratinocyte growth factor enhances *in vivo* retroviral-mediated gene transfer to mouse hepatocytes. J. Clin. Invest. 98, 2683–2687.

Caplen, N.J., Higginbotham, J.N., Scheel, J.R., Vahanian, N., Yoshida, Y., Hamada, H., Blaese, R.M., and Ramsey, W.J. (1999). Adeno-retroviral chimeric viruses as *in vivo* transducing agents. Gene Ther. 6, 454–459.

Chen, M., Kasahara, N., Keene, D.R., Chan, L., Hoeffler, W.K., Finlay, D., Barcova, M., Cannon, P.M., Mazurek, C., and Woodley, D.T. (2002). Restoration of type VII collagen expression and function in dystrophic epidermolysis bullosa. Nat. Genet. 32, 670–675.

Dandri, M., Burda, M.R., Torok, E., Pollok, J.M., Iwanska, A., Sommer, G., Rogiers, X., Rogler, C.E., Gupta, S., Will, H., Greten, H., and Petersen, J. (2001). Repopulation of mouse liver with human hepatocytes and *in vivo* infection with hepatitis B virus. Hepatology 33, 981–988.

De Vree, J.M., Ottenhoff, R., Bosma, P.J., Smith, A.J., Aten, J., and Oude Elferink, R.P. (2000). Correction of liver disease by hepatocyte transplantation in a mouse model of progressive familial intrahepatic cholestasis. Gastroenterology 119, 1720–1730.

Dorigo, O., Gil, J.S., Gallaher, S.D., Tan, B.T., Castro, M.G., Lowenstein, P.R., Calos, M.P., and Berk, A.J. (2004). Development of a novel helper-dependent adenovirus-Epstein-Barr virus hybrid system for the stable transformation of mammalian cells. J. Virol. 78, 6556–6566.

DuBridge, R.B., Tang, P., Hsia, H.C., Leong, P.M., Miller, J.H., and Calos, M.P. (1987). Analysis of mutation in human cells by using an Epstein-Barr virus shuttle system. Mol. Cell. Biol. 7, 379–387.

Emoto, C., Tateno, C., Hino, H., Amano, H., Imaoka, Y., Asahina, K., Asahara, T., and Yoshizato, K. (2005). Efficient *in vivo* xenogeneic retroviral vector-mediated gene transduction into human hepatocytes. Hum. Gene Ther. 16, 1168–1174.

Feng, M., Jackson, W.H., Jr., Goldman, C.K., Rancourt, C., Wang, M., Dusing, S.K., Siegal, G., and Curiel, D.T. (1997). Stable *in vivo* gene transduction via a novel adenoviral/retroviral chimeric vector [see comments]. Nat. Biotechnol. 15, 866–870.

Ferry, N., and Heard, J.M. (1998). Liver-directed gene transfer vectors. Hum. Gene Ther. 9, 1975–1981.

Graham, F.L., Smiley, J., Russell, W.C., and Nairn, R. (1977). Characteristics of a human cell line transformed by DNA from human adenovirus type 5. J. Gen. Virol. 36, 59–74.

Harui, A., Suzuki, S., Kochanek, S., and Mitani, K. (1999). Frequency and stability of chromosomal integration of adenovirus vectors. J. Virol. 73, 6141–6146.

Hofmann, W., Schubert, D., Labonte, J., Munson, L., Gibson, S., Scammell, J., Ferrigno, P., and Sodroski, J. (1999). Species-specific, postentry barriers to primate immunodeficiency virus infection. J. Virol. 73, 10020–10028.

Huard, J., Lochmuller, H., Acsadi, G., Jani, A., Massie, B., and Karpati, G. (1995). The route of administration is a major determinant of the transduction efficiency of rat tissues by adenoviral recombinants. Gene Ther. 2, 107–115.

Kass-Eisler, A., Falck-Pedersen, E., Elfenbein, D.H., Alvira, M., Buttrick, P.M., and Leinwand, L.A. (1994). The impact of developmental stage, route of administration and the immune system on adenovirus-mediated gene transfer. Gene Ther. 1, 395–402.

Katoh, M., Matsui, T., Nakajima, M., Tateno, C., Kataoka, M., Soeno, Y., Horie, T., Iwasaki, K., Yoshizato, K., and Yokoi, T. (2004). Expression of human cytochromes P450 in chimeric mice with humanized liver. Drug Metab. Dispos. 32, 1402–1410.

Kim, I.H., Jozkowicz, A., Piedra, P.A., Oka, K., and Chan, L. (2001). Lifetime correction of genetic deficiency in mice with a single injection of helper-dependent adenoviral vector. Proc. Natl. Acad. Sci. U.S.A. 98, 13282–13287.

Kochanek, S. (1999). High-capacity adenoviral vectors for gene transfer and somatic gene therapy. Hum. Gene Ther. 10, 2451–2459.

Korin, Y.D., and Zack, J.A. (1998). Progression to the G1b phase of the cell cycle is required for completion of human immunodeficiency virus type 1 reverse transcription in T cells. J. Virol. 72, 3161–3168.

Kubo, S., Kiwaki, K., Awata, H., Katoh, H., Kanegae, Y., Saito, I., Yamamoto, T., Miyazaki, J., Matsuda, I., and Endo, F. (1997). *In vivo* correction with recombinant adenovirus of 4-hydroxyphenylpyruvic acid dioxygenase deficiencies in strain III mice. Hum. Gene Ther. 8, 65–71.

Kubo, S., and Mitani, K. (2003). A new hybrid system capable of efficient lentiviral vector production and stable gene transfer mediated by a single helper-dependent adenoviral vector. J. Virol. 77, 2964–2971.

Leblois, H., Roche, C., Di Falco, N., Orsini, C., Yeh, P., and Perricaudet, M. (2000). Stable transduction of actively dividing cells via a novel adenoviral/episomal vector. Mol. Ther. 1, 314–322.

Li, Q., Kay, M.A., Finegold, M., Stratford-Perricaudet, L.D., and Woo, S.L. (1993). Assessment of recombinant adenoviral vectors for hepatic gene therapy. Hum. Gene Ther. 4, 403–409.

Lieber, A., He, C.Y., Meuse, L., Schowalter, D., Kirillova, I., Winther, B., and Kay, M.A. (1997). The role of Kupffer cell activation and viral gene expression in early liver toxicity after infusion of recombinant adenovirus vectors. J. Virol. 71, 8798–8807.

Lieber, A., Steinwaerder, D.S., Carlson, C.A., and Kay, M.A. (1999). Integrating adenovirus-adeno-associated virus hybrid vectors devoid of all viral genes. J. Virol. 73, 9314–9324.

Mariani, R., Rutter, G., Harris, M.E., Hope, T.J., Krausslich, H.G., and Landau, N.R. (2000). A block to human immunodeficiency virus type 1 assembly in murine cells. J. Virol. 74, 3859–3870.

Mercer, D.F., Schiller, D.E., Elliott, J.F., Douglas, D.N., Hao, C., Rinfret, A., Addison, W.R., Fischer, K.P., Churchill, T.A., Lakey, J.R., Tyrrell, D.L., and Kneteman, N.M. (2001). Hepatitis C virus replication in mice with chimeric human livers. Nat. Med. 7, 927–933.

Naldini, L., Blomer, U., Gallay, P., Ory, D., Mulligan, R., Gage, F.H., Verma, I.M., and Trono, D. (1996). *In vivo* gene delivery and stable transduction of nondividing cells by a lentiviral vector. Science 272, 263–267.

Nguyen, T.H., Oberholzer, J., Birraux, J., Majno, P., Morel, P., and Trono, D. (2002). Highly efficient lentiviral vector-mediated

transduction of nondividing, fully reimplantable primary hepatocytes. Mol. Ther. 6, 199–209.

Oka, K., Pastore, L., Kim, I.H., Merched, A., Nomura, S., Lee, H.J., Merched-Sauvage, M., Arden-Riley, C., Lee, B., Finegold, M., Beaudet, A., and Chan, L. (2001). Long-term stable correction of low-density lipoprotein receptor-deficient mice with a helper-dependent adenoviral vector expressing the very low-density lipoprotein receptor. Circulation 103, 1274–1281.

Ory, D.S., Neugeboren, B.A., and Mulligan, R.C. (1996). A stable human-derived packaging cell line for production of high titer retrovirus/vesicular stomatitis virus G pseudotypes. Proc. Natl. Acad. Sci. U.S.A. 93, 11400–11406.

Overturf, K., Al-Dhalimy, M., Tanguay, R., Brantly, M., Ou, C.N., Finegold, M., and Grompe, M. (1996). Hepatocytes corrected by gene therapy are selected *in vivo* in a murine model of hereditary tyrosinaemia type I. Nat. Genet. 12, 266–273.

Palmer, D., and Ng, P. (2003). Improved system for helper-dependent adenoviral vector production. Mol. Ther. 8, 846–852.

Park, F., Ohashi, K., Chiu, W., Naldini, L., and Kay, M.A. (2000). Efficient lentiviral transduction of liver requires cell cycling *in vivo*. Nat. Genet. 24, 49–52.

Parks, R.J., Chen, L., Anton, M., Sankar, U., Rudnicki, M.A., and Graham, F.L. (1996). A helper-dependent adenovirus vector system: Removal of helper virus by Cre-mediated excision of the viral packaging signal. Proc. Natl. Acad. Sci. U.S.A. 93, 13565–13570.

Patijn, G.A., Lieber, A., Schowalter, D.B., Schwall, R., and Kay, M.A. (1998). Hepatocyte growth factor induces hepatocyte proliferation *in vivo* and allows for efficient retroviral-mediated gene transfer in mice. Hepatology 28, 707–716.

Picard-Maureau, M., Kreppel, F., Lindemann, D., Juretzek, T., Herchenroder, O., Rethwilm, A., Kochanek, S., and Heinkelein, M. (2004). Foamy virus—adenovirus hybrid vectors. Gene Ther. 11, 722–728.

Recchia, A., Parks, R.J., Lamartina, S., Toniatti, C., Pieroni, L., Palombo, F., Ciliberto, G., Graham, F.L., Cortese, R., La Monica, N., and Colloca, S. (1999). Site-specific integration mediated by a hybrid adenovirus/adeno-associated virus vector. Proc. Natl. Acad. Sci. U.S.A. 96, 2615–2620.

Robbins, P.B., Skelton, D.C., Yu, X.J., Halene, S., Leonard, E.H., and Kohn, D.B. (1998). Consistent, persistent expression from modified retroviral vectors in murine hematopoietic stem cells. Proc. Natl. Acad. Sci. U.S.A. 95, 10182–10187.

Schiedner, G., Morral, N., Parks, R.J., Wu, Y., Koopmans, S.C., Langston, C., Graham, F.L., Beaudet, A.L., and Kochanek, S. (1998). Genomic DNA transfer with a high-capacity adenovirus vector results in improved *in vivo* gene expression and decreased toxicity. Nat. Genet. 18, 180–183.

Sena-Esteves, M., Saeki, Y., Fraefel, C., and Breakefield, X.O. (2000). HSV-1 amplicon vectors—simplicity and versatility. Mol. Ther. 2, 9–15.

Serafini, M., Naldini, L., and Introna, M. (2004). Molecular evidence of inefficient transduction of proliferating human B lymphocytes by VSV-pseudotyped HIV-1-derived lentivectors. Virology 325, 413–424.

Soifer, H., Higo, C., Kazazian, H.H., Jr., Moran, J.V., Mitani, K., and Kasahara, N. (2001). Stable integration of transgenes delivered by a retrotransposon-adenovirus hybrid vector. Hum. Gene Ther. 12, 1417–1428.

Soifer, H., Higo, C., Logg, C.R., Jih, L.J., Shichinohe, T., Harboe-Schmidt, E., Mitani, K., and Kasahara, N. (2002). A novel, helper-dependent, adenovirus-retrovirus hybrid vector: Stable transduction by a two-stage mechanism. Mol. Ther. 5, 599–608.

Tan, B.T., Wu, L., and Berk, A.J. (1999). An adenovirus-Epstein-Barr virus hybrid vector that stably transforms cultured cells with high efficiency. J. Virol. 73, 7582–7589.

Tateno, C., Yoshizane, Y., Saito, N., Kataoka, M., Utoh, R., Yamasaki, C., Tachibana, A., Soeno, Y., Asahina, K., Hino, H., Asahara, T., Yokoi, T., Furukawa, T., and Yoshizato, K. (2004). Near completely humanized liver in mice shows human-type metabolic responses to drugs. Am. J. Pathol. 165, 901–912.

Umana, P., Gerdes, C.A., Stone, D., Davis, J.R., Ward, D., Castro, M.G., and Lowenstein, P.R. (2001). Efficient FLPe recombinase enables scalable production of helper-dependent adenoviral vectors with negligible helper-virus contamination. Nat. Biotechnol. 19, 582–585.

Wivel, N.A., Gao, G.-P., and Wilson, J.M. (1999). Adenovirus vectors. In *The Development of Human Gene Therapy*. T. Friedmann, ed. (Cold Spring Harbor Laboratory Press, Cold Spring Harbor, NY) pp. 87–110.

Yant, S.R., Ehrhardt, A., Mikkelsen, J.G., Meuse, L., Pham, T., and Kay, M.A. (2002). Transposition from a gutless adenotransposon vector stabilizes transgene expression *in vivo*. Nat. Biotechnol. 20, 999–1005.

Address correspondence to:
Dr. Shuji Kubo
Laboratory of Host Defenses
Institute for Advanced Medical Sciences
Hyogo College of Medicine
1-1, Mukogawa-cho, Nishinomiya
Hyogo 663-8501
Japan

E-mail: s-kubo@hyo-med.ac.jp

Received for publication February 22, 2009;
accepted after revision September 2, 2009.

Published online: December 17, 2009.

Biochemical and Biophysical Research Communications 391 (2010) 316–321

Contents lists available at ScienceDirect

Biochemical and Biophysical Research Communications

journal homepage: www.elsevier.com/locate/ybbrc

Suppression of type I collagen production by microRNA-29b in cultured human stellate cells

Tomohiro Ogawa [a], Masashi Iizuka [a], Yumiko Sekiya [a,b], Katsutoshi Yoshizato [a,c], Kazuo Ikeda [d], Norifumi Kawada [a,*]

[a] Department of Hepatology, Graduate School of Medicine, Osaka City University, Osaka, Japan
[b] Toray Industries Inc., Kanagawa, Japan
[c] PhoenixBio Co. Ltd., Hiroshima, Japan
[d] Department of Functional Anatomy, Graduate School of Medicine, Nagoya City University, Aichi, Japan

ARTICLE INFO

Article history:
Received 6 November 2009
Available online 12 November 2009

Keywords:
Liver fibrosis
SP1
TGF-β
Interferon
TargetScan

ABSTRACT

MicroRNAs (miRNAs) are small noncoding RNAs that regulate gene expression through imperfect base pairing with the 3′ untranslated region (3′UTR) of target mRNA. We studied the regulation of alpha 1 (I) collagen (Col1A1) expression by miRNAs in human stellate cells, which are involved in liver fibrogenesis. Among miR-29b, -143, and -218, whose expressions were altered in response to transforming growth factor-β1 or interferon-α stimulation, miR-29b was the most effective suppressor of type I collagen at the mRNA and protein level via its direct binding to Col1A1 3′UTR. miR-29b also had an effect on SP1 expression. These results suggested that miR-29b is involved in the regulation of type I collagen expression by interferon-α in hepatic stellate cells. It is anticipated that miR-29b will be used for the regulation of stellate cell activation and lead to antifibrotic therapy.

Introduction

Hepatic stellate cells, which reside in the Disse's space outside the liver sinusoids, maintain a quiescent phenotype and store vitamin A under physiological conditions [1,2]. When liver injury occurs due to alcohol abuse, hepatitis viral infection, or obesity, stellate cells activate in response to inflammatory stimuli and become myofibroblastic cells that express smooth muscle α-actin as a representative marker [2]. Myofibroblastic cells secrete profibrogenic mediators, such as transforming growth factor-β (TGF-β), connective tissue growth factor, and tissue inhibitor of matrix metalloproteinases, and generate extracellular matrix materials including collagens, fibronectin, and laminin; thus, they play a pivotal role in liver fibrogenesis [3]. In particular, collagen production by activated stellate cells is regulated by TGF-β in an autocrine loop, which is accompanied by the induction of TGF-β receptors [4]. Suppression of hepatic stellate cell activation and collagen expression is thus a critical issue to establish therapeutic strategies for human liver fibrosis [1,5].

MicroRNAs (miRNAs) are endogenous small noncoding RNAs that modulate gene expression through imperfect base pairing with the 3′ untranslated region (UTR) of target mRNA, resulting in the inhibition of translation or the promotion of mRNA degradation [6,7]. miRNAs play roles in cell proliferation [8], development [9], and differentiation [10], and their contribution to human diseases such as cancer, cardiomyopathies, and schizophrenia have been reported [11–13]. miR-122 is also involved in the defense system against viral hepatitis C with regard to interferon (IFN)-β therapy [14], and miR-26 expression status is associated with survival and response to adjuvant IFNα therapy in patients with hepatocellular carcinoma [15]. Some miRNAs are involved in liver development and hepatocyte lipid metabolism [16–18].

Recent studies have shown that miRNAs are additionally involved in the alteration of hepatic stellate cell phenotypes; down-regulation of miR-27a and -27b allows culture-activated rat stellate cells to return to a quiescent phenotype with abundant vitamin A storage and decreased cell proliferation [19]; miR-15b and -16, which target the Bcl-2 and caspase signaling pathways, may affect stellate cell activation and liver fibrosis [20]. However, the function of miRNAs in hepatic stellate cell activation and their collagen production is largely unknown.

Here, we show that miR-29b, which is induced in human stellate cells (LX-2) treated with IFNα, is a potential regulator of type I collagen mRNA and protein expression. Although the primary action of IFNs is to eradicate viruses, i.e., hepatitis B and C viruses in

Abbreviations: Col1A1, alpha 1 (I) collagen; DMEM, Dulbecco's modified Eagle's medium; FBS, fetal bovine serum; IFN, interferon; miRNAs, microRNAs; TGF-β, transforming growth factor-β; UTR, untranslated region.

* Corresponding author. Address: Department of Hepatology, Graduate School of Medicine, Osaka City University, 1-4-3, Asahimachi, Abeno, Osaka 545-8585, Japan. Fax: +81 6 6646 9072.
E-mail address: kawadanori@med.osaka-cu.ac.jp (N. Kawada).

0006-291X/$ - see front matter © 2009 Elsevier Inc. All rights reserved.
doi:10.1016/j.bbrc.2009.11.056

the case of the liver, IFNs also exhibit an antifibrotic action in human chronic hepatitis [21,22] and rodent liver fibrosis models [23]. Our data suggest that miR-29b may be a novel regulator of type I collagen expression in addition to its involvement in the well-known Smad cascade. Moreover, miR-29b upregulation may play a partial role in the antifibrotic action of IFNs.

Materials and methods

Materials. Recombinant human TGF-β1 was purchased from PeproTech (London, UK). Human natural IFNα was obtained from Otsuka Pharmaceutical Co. (Tokushima, Japan). Precursors of miR-29b, -143, and -218, and the negative control were purchased from Ambion (Austin, TX, USA). Dulbecco's modified Eagle's medium (DMEM) and fetal bovine serum (FBS) were purchased from Sigma Chemical Co. (St. Louis, MO, USA). Rabbit monoclonal antibodies against Smad2 and phospho-Smad2 were purchased from Cell Signaling Technology Inc. (Beverly, MA, USA). The mouse monoclonal antibody against SP1 was purchased from Bio Matrix Research Inc. (Chiba, Japan). Rabbit polyclonal antibody against type I collagen was purchased from Rockland Immunochemicals, Inc. (Gilbertsville, PA, USA). Mouse monoclonal antibody against GAPDH was purchased from Chemicon International Inc. (Temecula, CA, USA). Enhanced Chemiluminescence plus detection reagent was purchased from GE Healthcare (Buckinghamshire, UK). Immobilon P membranes were purchased from Millipore Corp. (Bedford, MA, USA). All other reagents were purchased from Sigma Chemical Co. or Wako Pure Chemical Co. (Osaka, Japan).

Preparation of the human hepatic stellate cell line LX-2. The human hepatic stellate cell line (LX-2, donated by Dr. Scott Friedman), which was spontaneously immortalized by growth in low serum, was established as reported previously [24]. Characterizations of the cells are described in detail elsewhere. The cells were maintained on plastic culture plates in DMEM supplemented with 10% FBS. After the culture had continued for the indicated number of days, the medium was replaced with DMEM supplemented with 0.1% FBS plus test agents, and the culture was continued for another 24 h.

Quantitative real-time PCR. Total RNA was extracted from human stellate cells using the miRNeasy Mini Kit (Qiagen, Valencia, CA, USA). cDNAs were synthesized using 0.5 μg of total RNA, ReverTra Ace (Toyobo, Osaka, Japan), and oligo(dT)$_{12-18}$ primers according to the manufacturer's instructions [25]. Gene expression was measured by real-time PCR using cDNA, real-time PCR Master Mix Reagents (Toyobo), and a set of gene-specific oligonucleotide primers (alpha 1 (I) collagen [Col1A1]: Forward 5′-CCCGGGTTTCAGAGACA ACTTC-3′, Reverse 5′-TCCACATGCTTTATTCCAGCAATC-3′; TGF-β1: Forward 5′-AGCGACTCGCCAGAGTGGTTA-3′, Reverse 5′-GCAGTG TGTTATCCCTGCTGTCA-3′; SP1: Forward 5′-TCGGATGAGCTACA GAGGCACAA-3′, Reverse 5′-GTCACTCCTCATGAAGCGCTTAGG-3′; and GAPDH: Forward 5′-GCACCGTCAAGGCTGAGAAC-3′, Reverse 5′-TGGTGAAGACGCCAGTGGA-3′) with an Applied Biosystems Prism 7500 (Applied Biosystems, Foster City, CA, USA). To detect miRNA expression, the RT reaction was performed using the TaqMan MicroRNA Assay (Applied Biosystems) according to the manufacturer's instructions. The GAPDH level was measured and used to normalize the relative abundance of mRNAs and miRNAs.

Immunoblot. Proteins (20–50 μg) were subjected to sodium dodecyl sulfate–polyacrylamide gel electrophoresis and then transferred onto Immobilon P membranes. After blocking, the membranes were treated with primary antibodies, followed by peroxidase-conjugated secondary antibodies. Immunoreactive bands were visualized by the enhanced chemiluminescence system using the Fujifilm Image Reader LAS-3000 (Fuji Medical Systems, Stamford, CT, USA).

Transient transfection of miRNA precursors. Precursors of miR-29b, -143, and -218, and the negative control were transfected into human stellate cells using Lipofectamine 2000 (Invitrogen, Carlsbad, CA, USA) at a final concentration of 50 nM. Briefly, the cells were plated in DMEM supplemented with 10% FBS at a density of 1–2 × 10^5 cells/ml 24 h prior to the transfection. miRNA precursors and Lipofectamine 2000 were mixed at a ratio of 25 (pmol):1 (μl) in Opti-MEM I Reduced Medium (Invitrogen) and incubated for 20–30 min at room temperature. The miRNA precursor–Lipofectamine 2000 complexes were then added to stellate cell culture medium. After 6 h, the culture medium was changed, and TGF-β1 was added at a concentration of 2 ng/ml.

Luciferase reporter assay. 3′UTRs containing putative miRNA target regions of the Col1A1 and SP1 genes were obtained by PCR using human stellate cell cDNA as a template and primer sets as follows: Col1A1–miR-29: Forward 5′-TTCTCGAGGTTCTTGTCTTG ATGTGTCACC-3′, Reverse 5′-TTTCTAGAGAGAGCAGAGGCCTGAGA AG-3′; Col1A1–miR-143: Forward 5′-CTCGAGACTCCCTCCATCCCAA CCT-3′, Reverse 5′-TCTAGAATTGCTGGGCAGACAATAC-3′; Col1A1–miR-218: Forward 5′-CTCGAGGTGGATGGGGACTTGTGAAT-3′, Reverse 5′-TCTAGATTATGTTTGGGTCATTTCCAC-3′; SP1–miR-29: Forward 5′-TTCTCGAGTGGGTGCTACACAGAATGC-3′, Reverse 5′-TTTC TAGAAGACTGTCCTTATTTCCTTGGTA-3′; and SP1–miR-218: Forward 5′-CTCGAGGATGTTTTCCCTTAACTTTTCCT-3′, Reverse 5′-TCT AGACTAAAAGCTTATATCCTCAGCATC-3′. Each of the forward and reverse primers carried the *Xho*I and *Xba*I sites at their 5′-ends. The obtained DNA fragments were inserted into the pmirGLO Vector (Promega, San Luis Obispo, CA, USA). The resulting vectors were dubbed pCol1A1–miR-29/mirGLO, pCol1A1–miR-143/mirGLO, pCol1A1–miR-218/mirGLO, pSP1–miR-29/mirGLO, and pSP1–miR-218/mirGLO. Human stellate cells were seeded on 96-well plates (Microtest 96-well Assay Plate; Becton Dickinson, Franklin Lakes, NJ, USA) in DMEM supplemented with 10% FBS at a density of 2 × 10^4 cells/well. The following day, they were transfected with 200 ng of reporter plasmid along with miRNA precursors using Lipofectamine 2000 as described above and incubated for an additional 24 h. After incubation, the medium was removed from the wells, and 20 μl of phosphate-buffered saline was added. The Dual-Glo Luciferase Assay System (Promega) was used to analyze luciferase expression according to the manufacturer's protocol. Firefly luciferase activity was normalized to *Renilla* luciferase activity to adjust for variations in transfection efficiency among experiments.

Statistical analysis. Data presented as bar graphs are the means ± SD of at least three independent experiments. Statistical analysis was performed using Student's *t*-test, and $P < 0.05$ was considered significant.

Results and discussion

Regulation of Col1A1 expression by TGF-β1 and IFNα in human stellate cells

Immortalized human stellate cells, LX-2, are classified as an activated phenotype that expresses mRNAs for Col1A1 and other fibrogenetic molecules and are reported to be highly gene-transfectable [24]. At first, we observed that Col1A1 mRNA expression increased dose-dependently by TGF-β1 (Fig. 1A), whereas this upregulation was significantly inhibited by the presence of 100 IU/ml of human IFNα (Fig. 1B).

Extraction of miR-29b, -143, and -218 as candidates interacting with Col1A1 3′UTR

To determine the role of miRNAs in human stellate cell collagen expression, we searched for predictable miRNAs that could interact